Arab American University

Faculty of Graduate Studies

Pedestrian Dynamics: Experimental Investigation of the Fundamental Diagram Across Cultures

By

Rudina Munjid Sudqi Subaih

Main Supervisor
Dr. Mohammed A. M. Maree
Co-Supervisor
Dr. Mohcine Chraibi

This thesis was submitted in partial fulfillment of the requirements for the Master's degree in Computer Science
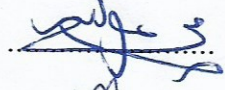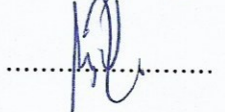
January/ 2020

Pedestrian Dynamics: Experimental Investigation of the Fundamental Diagram Across Cultures

By

Rudina Munjid Sudqi Subaih

This thesis was defended successfully on **06/01/2020** and approved by:

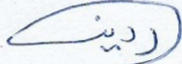| Committee members	Signature
1. Supervisor Name: Dr. Mohammed Maree	
2. Co-Supervisor Name: Dr. Mohcine Chraibi	
3. Internal Examiner Name: Dr. Amjad Rattrout	
4. External Examiner Name: Dr. Yousef Daraghmeh	

Declaration

This is to declare that the thesis entitled "Pedestrian Dynamics: Experimental Investigation of the Fundamental Diagram Across Cultures" under the supervision of Dr. Mohammed A. M. Maree and Dr. Mohcine Chraibi is my own work and does not contain any unacknowledged work or material previously published or written by another person, except where due reference is made in the text of the document.

Date: 20 /06/ 2020

Name: Rudina Munjid Sudqi Subaih   Signature:

Acknowledgments

I would like to express my sincere gratitude to people who always stand beside me during my master's journey, foremost, my thesis supervisors Dr. Mohammed A. M. Maree from Arab American University and Dr. Mohcine Chraibi from Institute for Advanced Simulation- Civil Safety Research (IAS-7) in Forschungszentrum Jülich research center, Germany. They always exist to give me priceless advices and their total support. I learned from them how to be consistent and persistent toward exemplary work.

Many thanks to Prof. Dr. Armin Seyfried, Head of the IAS-7 institute, and my colleagues for their great support and teamwork. Without their support, my research could not have been successfully conducted. Also, sincere thanks to Mr. Sami Awad, and the students from Arab American University – Palestine for their assistance by volunteering to participate in the conducted experiments. Thanks for giving me your time and efforts to accomplish this great work.

I must express my very profound gratitude to my parent; my lovely mother for her unlimited support, and my lovely father, my first teacher whose soul is always besides me and gives me the strength to continue. My beloved sister and brothers: Ala, Suhail, Diya, Hiba, Basim, and Basil, thank you for standing beside me and for your continuous encouragement throughout my years of study. They tolerate my ambitious, curiosity, and my continuous seeking for completeness. My success needs your generous support.

Abstract

The dynamics of pedestrians are normally controlled and influenced by several factors that shape the flow, velocity, and density of various pedestrian groups. Some of these factors are related to pedestrian compositions. Over the past few years, several experimental studies have been conducted to identify and understand the impact of such factors on pedestrian movement characteristics. Among the most important experiments have been carried out in an attempt to investigate the dynamics of pedestrians in narrow corridors with closed boundary conditions. The advantage of this simplified set-up is the ease to control the density, which enables studying the so-called Fundamental Diagram (density-velocity relation, FD) in a controlled and consistent manner. The goal of this research is to investigate the physical movement characteristics of Palestinian pedestrians using the density-velocity, velocity-headway, and density-headway relations for single-file movement experiments conducted with an emphasis on various gender compositions. We compared the experiment findings against similar experiments that have been conducted in other cultures, namely in Germany and India. Moreover, we perform a comparative analysis concerning the age factor, by comparing our results with two types of experiments that have been conducted in China: young, and old pedestrians. After identifying the factors that control the dynamics of pedestrians, we used them to investigate the impact of each factor on the movement decisions and further predict future movement characteristics using artificial neural networks. Our proposed model precisely forecasts future velocities and headway distances for various pedestrian compositions and densities for single-file movement experiments. The proposed prediction model was validated using two trajectory datasets from Palestine and China.

Table of Contents

List of Tables

List of Figures

List of Abbreviations

FD: Fundamental Diagram.

PD: Pedestrian Dynamic.

FFNN: Feedforward Neural Network.

MLP: Multi-layer Perceptron.

Chapter 1 — Introduction

1.1 Motivation

Walking is an innate method to move from one place to another in human life. Usually, people used to walk in different manners to reach any place because every person is unique and has her/his movement characteristics. For instance, each pedestrian belongs to a culture that has its social conventions, common-sense rules, and beliefs. Also, pedestrians walk in different environments (every place has its scene semantics) and they have their properties (gender, age, weight, length). Consequently, modeling pedestrian dynamics is crucial to understand these different characteristics and the complex interactions between people in the crowds. Understanding the factors that impact pedestrian dynamics - Figure 1.1 shows some of these factors - is important and valuable for a broad range of applications such as developing socially-aware robots (Randhavane et al., 2019), building autonomous vehicle navigation systems (Rasouli & Tsotsos, 2019), buildings and stations design (Dubroca-Voisin, Kabalan, & Leurent, 2019), planning and designing mass gathering facilities (Owaidah, Olaru, Bennamoun, Sohel, & Khan, 2019), and abnormal behavior detection (Tay, Connie, Ong, Goh, & Teh, 2019). For this purpose, various experimental, modeling, and simulation studies in the Pedestrian Dynamic (PD) field have been focusing on these emergent properties during the movement for different situations.
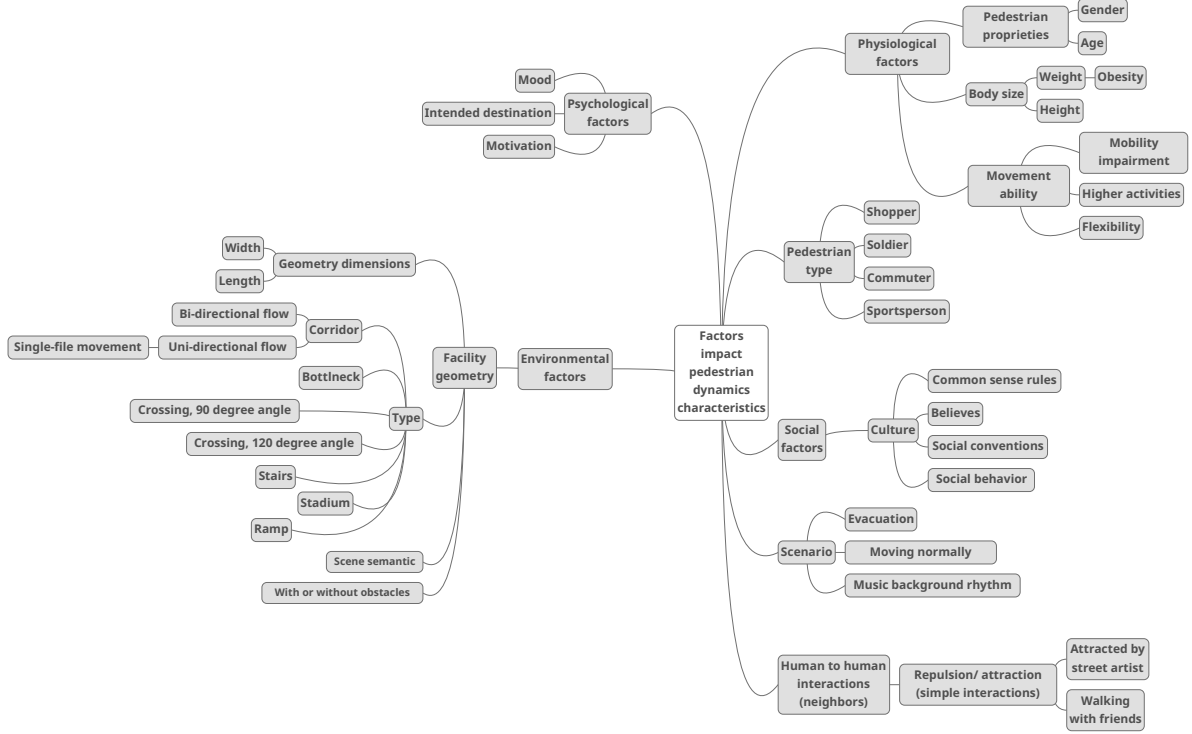
Figure 1.1: Some of the factors that impact PD characteristics classified after reviewing the literature.

Inspired by the experimental studies that have been conducted to investigate the influential factors that control the dynamics of pedestrians in Germany and India, we aim to investigate the PDs of the targeted culture. This research analyzes the main movement characteristics of pedestrians on single-file movement namely in Palestine. The advantages of this simplified set-up are the ease to control the density and acquire pedestrian trajectory data. Furthermore, this type of experiment conducted in different countries e.g. Germany, China, and India, which offers the possibility to adequately compare the results and scrutinize the influence of culture on the FD. Additionally, in this research, we focus on pedestrian compositions in the crowd. Pedestrian compositions are among the main factors that influence the movement of pedestrians. Accordingly, various compositions are realized based on gender, social conventions, and age. Laboratory experiments that investigate PDs give us the chance to analyze the key dynamic parameters, by applying the appropriate settings in narrow corridors with closed boundary conditions. Moreover, based on the experimental results, we propose a neural network prediction model to predict the movement characteristics (velocity, headway) of different pedestrians. The data

extracted from our single-file movement experiments and their corresponding data obtained from the Chinese experiments (Cao, Zhang, Song, Shi, & Zhang, 2018) is used in training and validating the model. The proposed prediction model helps to forecast the velocity and headway for the different densities of the single-file movement experiments with different pedestrian compositions.

1.2 Problem Statement

As we have discussed previously, the dynamics of pedestrians are normally influenced by several factors. These factors could be social (common-sense rules, social conventions), environmental (obstacles, scene semantics), physiological (weight, length), and psychological (mood) factors. When people walk on streets, malls, or corridors, they usually try to follow social conventions and common-sense behavior to retain their comfort zone and avoid accidents. For instance, when a person walks she/he thinks about the appropriate next step to reach the destination without colliding with others by respecting their personal space (a.k.a. comfort zone). Understanding these social and behavioral aspects can lead to developing various useful applications that assist people in different application domains.

Until now, there is no experimental study performed to study the dynamic characteristics of pedestrians across the Arab culture in general, and in Palestine in particular. Also, there is little attention that has been given to experimental studies that investigate the movement characteristics of different gender compositions including male, female, and mixed groups. Furthermore, there is no comprehensive study focusing on pedestrian compositions based on gender, culture, and age factors together. In this section we present the research questions that we will address during our research work:

1. What are the differences between the movement characteristics of female and male pedestrians?

2. How the composition of pedestrians - based on gender, culture, and age - impact the way people walk?

3. Do Palestinian pedestrians walk differently than pedestrians in other cultures such as

German, Indian, and Chinese pedestrians?

4. How the movement of people of different ages vary?

5. What are the crucial factors that can influence future pedestrians' movement behavior considering various pedestrian compositions?

6. Can we predict the factors - based on manually-collected trajectory data - that play significant roles in designing future pedestrian-aware devices and facilities?

To answer these questions, we performed unidirectional flow (single-file movement) experiments to investigate the movement characteristics of Palestinian pedestrians. Unidirectional flow is the primary aspect of pedestrians' motion. Motion data - the trajectories of pedestrians that are acquired from the experiments – are captured, extracted and analyzed to mainly study the Fundamental Diagram (FD). The FD (velocity-density relation) describes the movement of pedestrians and forms the main input for designing PD related applications. Accordingly, we conduct a comparative analysis to investigate the main characteristics of PDs observed from our experiments and other experiments based on various pedestrian compositions. This comparative analysis assists in a better understanding of the main factors that drive the dynamics of pedestrians across different cultures, as well as in developing intelligent computational applications, that correspond with cultural, social and behavioral characteristics of PDs. Furthermore, we used the data and the analysis results of these experiments to build a Feedforward Neural Network (FFNN) model to predict the dynamic characteristics of pedestrians inside different crowd densities, specifically for single-file movement set-ups.

1.3 Research Steps

The following points summarize the main steps that we have carried out during our research:

- **Pre-experiment and Actual Experiment Phases**

  Three pre-experiments were conducted with three pedestrians to adjust camera settings and prepare the location of the experiments. The movement of pedestrians during their walking was captured using video cameras from the side view. Next, we performed the

main experiments based on the optimized settings focusing on the gender factor. Both female and male pedestrians participated in these experiments. All pedestrians are university students volunteered to participate in the experiments. We divided the experiments into different runs with various pedestrian densities.

- **Data Collection and Extraction**

  This phase comes after capturing the video footage from the main experiments. PeTrack software (Boltes & Seyfried, 2013) was used to track and extract pedestrian trajectories (x and y positions during different time frames). The result of this phase is a collection of *.txt* files that contains the IDs of the video frames, pedestrians' IDs, x and y position coordinates, and pedestrians' proprieties (gender, length).

- **Code Implementation and Experimental Evaluation**

  The resulting trajectory files from the previous phase were utilized in the data analysis and evaluation phase. In this phase, we developed a python code to calculate the density, velocity, and headway of different pedestrians during different time frames. Different movement characteristics were taken into account during the calculations. Moreover, two different measurement methods (Classical and Voronoi) were used to measure these quantities. Finally, we plotted the FD (density-velocity), density-headway, and headway-velocity relations to compare the results based on gender, culture, and age factors.

- **Prediction Model**

  At this phase, we proposed exploiting a FFNN prediction model to predict main movement quantities (velocity and headway). We used the trajectories and the results from the Palestinian and Chinese single-file movement experiments to build the proposed prediction model.

1.4 Contributions

We summarize the main contributions of the research as follows:

1. Introducing an empirical dataset that comprises Palestinian pedestrians' motion data collected in narrow corridors with closed boundary conditions.

2. Investigating and comparing the main characteristics of PDs observed from the experimental data for different countries including Palestine based on various pedestrian compositions.

3. Conducting a comparative analysis based on gender and age factors to investigate if there are differences in movement behaviors across pedestrians of different ages and genders.

4. Designing and implementing a FFNN model that predicts PD characteristics, namely velocity and headway.

In this section, we also list the accepted publications:

1. Paper entitled "Gender-based Insights into the Fundamental Diagram of Pedestrian Dynamics". In this paper, we described in detail our single-file movement gender-based laboratory experiments performed in Palestine. Then the main characteristics of female and male PDs were investigated by conducting a comparative analysis among the gender-based FDs for different cultures, in an attempt to study the different characteristics and factors that may influence their dynamics and motion flows.

2. (Accepted: 08 January 2020) The second paper, entitled " Experimental Investigation on the Alleged Gender-differences in Pedestrian Dynamics: A Study Reveals No Gender Differences in Pedestrian Movement Behavior ". In this paper, we analyzed the movement characteristics of Palestinian pedestrians using the FD for single-file movement experiments conducted with an emphasis on gender compositions. We compared the FDs of different gender compositions: male only, female only, and mixed-gender composition. We also compared Palestinian experiment findings against other culture-based experiments to demonstrate that pedestrian cultures influence on their movement characteristics. Moreover, we demonstrate that age is another factor that influences pedestrians' movement. A comparative analysis is performed between Palestinian and Chinese experiments to signify this factor.

References:

- Subaih R., Maree M., Chraibi M., Awad S., Zanoon T. (2019) Gender-based Insights into the Fundamental Diagram of Pedestrian Dynamics. In: Nguyen N., Chbeir R., Exposito E., Aniorté P., Trawiński B. (eds) Computational Collective Intelligence. ICCCI 2019. Lecture Notes in Computer Science, vol 11683. Springer, Cham.

- Subaih R., Maree M., Chraibi M., Awad S., Zanoon T. (2020) Experimental Investigation on the Alleged Gender-differences in Pedestrian Dynamics: A Study Reveals No Gender Differences in Pedestrian Movement Behavior. In: IEEE ACCESS Journal, Impact Factor = 4.098. SJR 0.61, Q1, H-index 56.

1.5 Structure of the Thesis

The rest of this thesis is organized as follows. In Chapter 2, we review the literature related to the subject of our study. Chapter 3 describes the conducted experiments and data extraction procedures. In Chapter 4, the measurement methods used to calculate the movement quantities such as density, velocity, and headway are presented. In Chapter 5, we analyze the results of our experiments and compare them against those obtained from similar experiments considering the gender, culture, and age factors. In Chapter 6, we introduce our proposed FFNN prediction model and discuss the produced results. Finally, in Chapter 7, the conclusions and outline the future directions of our research work are outlined.

Chapter 2 — Literature Review

2.1   Introduction

Over the past few years, various types of research have been carried out in an attempt to investigate the main influential factors that have an impact on pedestrians' movement and shape the PD characteristics from different perspectives (Jin, Jiang, Li, & Li, 2019; Ren, Zhang, Song, & Cao, 2019; Zeng et al., 2019; Boltes, Zhang, Tordeux, Schadschneider, & Seyfried, 2019; Xiao et al., 2019; Cao et al., 2018; J. Zhang, 2012; Chattaraj, Seyfried, & Chakroborty, 2009; Seyfried, Steffen, Klingsch, & Boltes, 2005). This interdisciplinary field has continued to be the focus of many researchers from different backgrounds. For instance, some researchers focused on PD experiments to investigate the influence of different factors such as background music (Zeng et al., 2019), pedestrian age (Ren et al., 2019; Cao et al., 2016, 2018), and culture (Chattaraj et al., 2009) in movement characteristics. While others consider implementing algorithms and techniques that can assist in predicting future pedestrian behaviors (Tordeux, Chraibi, Seyfried, & Schadschneider, 2019; Hasan et al., 2018; Xue, Huynh, & Reynolds, 2017; Tkachuk, Song, & Maltseva, 2018). Accordingly, we discuss the literature review chapter in terms of two main aspects. First, we provide a review of observational and empirical researches in the PD field, and then we review several research works that have focused on PD prediction and simulation models that aim to predict and simulate various PD characteristics.

2.2   Pedestrian Dynamics: Observational Studies and Experimental Perspectives

Various studies have explored the factors that influence PD characteristics in the crowds (Jin et al., 2019; Ren et al., 2019; Zeng et al., 2019; Boltes et al., 2019; Xiao et al., 2019; Cao et al., 2018; J. Zhang, 2012; Chattaraj et al., 2009; Seyfried et al., 2005). Some of these studies are observational focusing on monitoring PDs to investigate their movement characteristics, while

others rely on laboratory experiments to analyze movement quantities by controlling the factors that may impact pedestrians' movement.

For instance, Tanaboriboon et al. (Tanaboriboon & Guyano, 1991) investigated the dynamics of Bangkok, Thailand pedestrians by collecting speed data from different public areas for various walkways: stairways, sidewalks, and crosswalks using a video camera. They compared the walking rates of Bangkok pedestrians with other pedestrians from Western (England, United States, Canada) and other Asian countries (Saudi Arabia, India, Thailand, Singapore, Sri Lanka). The results confirmed that the mean walking speed of Thailand pedestrians is less than Western countries and relatively like the mean walking speed of other Asian pedestrians. Another observational study, (Finnis & Walton, 2008) conducted in New Zealand investigated the impact of environmental and personal factors on the mean walking speeds of New Zealand pedestrians under different environmental conditions: rural, urban, and gradient townships. The results showed that there is an interrelationship between mean walking speed and environmental factors, personal characteristics of pedestrian, and physical factors. Meanwhile, there is no relationship between the mean walking speed of pedestrians and the population size. However, in the aforementioned studies, the mean speed of pedestrians was averaged (traveled distance over the traveling time) resulting in a degraded level of accuracy for describing pedestrian movement on a microscopic level. Besides, the speed of different pedestrian types was measured in a general way without careful isolation and investigation of the individual factors that may affect their speed. Furthermore, data obtained from these experiments were acquired manually; leading to inaccuracies in the extraction of trajectories. Another study (Morrall, Ratnayake, & Seneviratne, 1991) aimed at investigating the cultural differences between Sri Lanka and Canada. The dynamics quantities including density, velocity, and flow of different sidewalk widths were investigated. However, the study focused only on low-density dynamic data, and the quantities of interest were collected manually using a time-lapse photography technique instead of using a precise automatic data extraction technique.

On the other hand, other PD studies relied on performing laboratory experiments to study pedestrian flow features. Diverse experiments with different configurations and purposes have been conducted in this context. Some of them are used to study the microscopic (focus on individ-

ual pedestrian) movement characteristics, while others investigate the macroscopic (focus on general crowd flow) movement characteristics. The trajectory data is accordingly analyzed to investigate the microscopic characteristics such as the individual mean density, individual mean velocity, and headway (distance to move forward). Also, the macroscopic characteristics such as average velocity, average density, flow, and self-organization phenomena - is pattern-formation processes are formed between pedestrians inside the crowds; it includes stop-and-go-waves, lateral oscillations, jamming, congestion, zipper effect, and lane formation - are studied.

Among the PD studies, there are single-file movement experiments. The configuration of these experiments is designed in a way that allows pedestrians to move inside a pre-designed set-up in the same direction (unidirectional) without overtaking. This type of experiments is very important to study the essence and the main characteristics of the flow. For instance, Zeng at el. (Zeng et al., 2019) aimed to investigate the impact of background music on pedestrians' movement. As stated by the authors, music rhythms have been found to contribute to the improvement of the pedestrian flow. To carry out the experiments, twelve runs were conducted in Hefei, China and six of them with different background music (with different rhythm ranges) and the other six were conducted under the normal conditions (without music). The set-up included an oval corridor with a central circumference of 21.93 m, straight parts of length about 5 m, corridor width about 0.8 m, and measurement section of length 3.5 m. Forty college students were involved in this experiment (18 males, and 22 females). Runs included variable numbers of pedestrians $N = 2$, 5, 10, 20, 30, 40 and the global density ranges were between 0.09 m^{-1} to 1.82 m^{-1}. The experiments were captured, and the trajectory data extracted using PeTrack software (Boltes & Seyfried, 2013). By analyzing the trajectory data, the FD, time-space diagram, and stepping behavior, the authors have observed the following results:

1. With background music, the flow and velocity were the same as normal movement conditions (without music) when the density less than 1 m^{-1}, while it's less than normal conditions when for high densities (density more than 1 m^{-1}).

2. Stop-and-go-waves with music are more frequent than in normal movement conditions due to the higher stopping and restarting of movement.

3. The stopping duration of pedestrians is longer with music 15.96 sec - it's about 6.52 sec without music -, so it could be considered as a factor for jam formation.

4. At high density, The stepping frequency decrease with rhythm - the step frequency under the normal conditions is about 120 steps/min -.

5. There is no effect for the music on the step length.

Another single-file movement study conducted by Ren et al. (Ren et al., 2019) has focused on the age factor. In this study, straight corridor unidirectional flow laboratory experiments were performed in Hefei, China to study the movement characteristics of elders under different densities. Seventy-three pedestrians of mean age 64.7 years old have volunteered in these experiments. The trajectories were extracted using PeTrack software and then analyzed using Voronoi method to calculate the velocity and density of pedestrians. The performed experiments included nine different scenarios by changing the corridor entrance and exit widths to achieve different densities during the experiments. The results were compared with the young pedestrian experiments conducted in Germany (J. Zhang, Klingsch, Schadschneider, & Seyfried, 2011) and showed that there was a marked difference between elders and young movement proprieties. Elders walk slower than young pedestrians with a free-flow speed 1.28 ms^{-1} and small step size, and they keep a larger distance to the wall than the youth.

In another experiment conducted by Cao et al. (Cao et al., 2016), the authors aimed at investigating the properties of different age compositions: young, old, and mixed (young, old) pedestrians. To do this, a single-file movement experiment was carried out in Tianshui Health school, Gansu, China. The set-up included an oval corridor with an outer and inner radius about 2.9 m and 2.1 m respectively, and with a length of 25.7 m and width of 0.8 m. One hundred twenty-seven pedestrians participated in the experiment, where eighty of them are young students with an average age of 17 years and the rest (47 pedestrians) are old with an average age of 52 years. The global density ranged between 0.19 m^{-1} and 2.33 m^{-1}. All runs were filmed from the top view using a video camera and then the videos were further processed to extract the trajectory of pedestrians using PeTrack software. The authors focused on the 1-D properties of PDs by investigating the longitudinal interactions among pedestrians. Thus, they used the

individual velocity and density to plot the relation of dynamic quantities. In the beginning, the time-space diagram was studied, and the authors found out that the movement properties and self-adaptive abilities of different age groups differ; the jamming and stop-and-go waves occur more frequently in mixed groups than the young group. Moreover, they studied the FD (density-velocity relation) for different age groups and for different parts of the experiment geometry. It was found that there are no differences observed between the pedestrian macroscopic propri-eties - mean density and mean velocity - if she/he moves in straight paths or curves. But the age composition of pedestrians has an impact on the FD. However, young pedestrians move faster than old and the mixed age pedestrian groups. Furthermore, for velocity-headway relation the authors found out three linear regimes on young, old, and mixed pedestrian groups as follows:

1. Free regime: where the individual mean velocity is independent of the headway distance. This regime appears on the headway-velocity relation of young pedestrian, old pedestrian, and mixed-age pedestrian experiments.

2. Weakly constrained regime: where the individual mean velocity depends weakly on the headway distance. This was observed in the old and mixed-age compositions.

3. Strongly constrained regime: where the individual mean velocity depends on the headway distance. This was seen in young and mixed groups but was not clear for old pedestrian experiments because of the lack of high-density experiments.

Using the same experiment, Cao et al. investigated the stepping behavior of different age groups (Cao et al., 2018). In this context, velocity-step length and velocity-step width relations were analyzed. Also, the effect of gender and height of the pedestrian on the step length and funda-mental diagram were studied. The results show that in the velocity-step width relation diagram, there are two stages for young, old, and mixed age groups. The first is the constrained walking stage were the step width decrease with the increment of longitudinal velocity and the smaller longitudinal velocity causes a larger step width. In addition, in high-density situations, the pedestrians prefer to sway in two lateral directions instead of stopping. In the second stage, the free walking stage, the pedestrians move with their free velocity and the step width almost doesn't change. At all times, the step widths of elders are larger than the young pedestrians.

Moreover, the average step width for all age groups under the free walking conditions is between 5 cm to 8 cm. For the velocity-step length relation, it's been found that for all age groups the step length increases with the increase of the velocity. Finally, the authors investigated the effect of gender and pedestrian height on the step length and FD for both young and old groups. The males and taller pedestrians have long step length. On the contrary, gender and length don't have obvious influence on the FD.

Another study by Chattaraj et al. (Chattaraj et al., 2009) considered the influence of culture factor and length of the corridor on pedestrians' movement behavior. The authors compared the FDs and dynamic characteristics of pedestrians from two countries: Germany (mixed), and India (males). The results showed that different movement properties characterize pedestrians of each culture. For instance, Indians walk faster than Germans and have felt more comfortable in relatively high-density situations. Additionally, the authors studied the effect of the corridor length on the headway-velocity and FD relations. The relation were studied for two corridor lengths (17.3 m, 34.6 m) for India experiments. By testing the relations statically, it is found that the length of the corridor has no impact on the headway-velocity relation.

In a similar line of research, Cheng-Jie Jin et al. (Jin et al., 2019) performed single-file movement experiments in the Jiulonghu Campus of Southeast University China to investigate unidirectional pedestrian flow under high-density situations with a maximum global density of 4 m^{-1}. Two hundred and three pedestrians were involved in the experiments. Participants were distributed across seven runs: A, B, C, D, E, F, and G, with numbers of pedestrians $N =$ 49, 71, 108, 121, 152, 180, 203 respectively. The experiment used a circular set-up with an inner and outer radius of 7.8 m, 8.2 m respectively, and corridor width of 0.4 m to enforce the single movement and prevent overtaking. The pedestrians during each run passed through the pathway and their movement was captured using Unmanned Aerial Vehicle (UAV) hover the circular set-up with height 25 m. Then, the microscopic data was extracted from the videos using Tracker software (*Tracker video analysis and modeling tool*, n.d.). First, the authors conducted an intercultural comparison with German and Indian culture-based (Chattaraj et al., 2009; Seyfried et al., 2005) single-file movement experiments. The results of comparing the FDs (velocity-density relation) showed that the velocities of Chinese are close to the velocities

of Indian pedestrians and higher than German pedestrians. Besides, The flow rate of Chinese was close to Indians and larger than Germans. This result was explained by cultural differences since both Chinese and Indians are in general used to move in relatively more populated spaces than their German counterparts. Second, the authors presented the FD (density-flow relation) of the experiments using two methods:

1. Local values: they divided the set-up to subareas, and then calculated the density and flow for each subarea. Data points of local values were averaged over the density interval of 0.2 ped/m to plot the relation.

2. Global values: density here was fixed for all the set-up (the number of pedestrians divided by the circular path length). The flow used was the average flow of all 8 subareas. The data points of the relation corresponded to each run.

By plotting the relation diagram, it has been found that the flow rates decrease with the increases of density (the global results coincide with the local results). Also, the flow during the time in high-density run G is stable at the beginning, because the pedestrians did not move at the beginning. This phase named " Warm-up time " took 3 minutes until the pedestrians started to walk after adaptation. Third, time-headway distribution was investigated to measure the time that pedestrian needs to pass through a " Virtual loop detector " which is a virtual circular pathway determined in the set-up. The results of the experiments were categorized into three groups based on different peak times:

1. First group: the peak is reached when the time between is 1 sec. to 1.25 sec.. This included A and B runs.

2. Second group: the peak starts to occur when the time is between 2 sec. to 2.25 sec. This included C and D runs.

3. Third group: there was no peak during the runs. This included E and F runs because the high number of pedestrians in these two runs.

Finally, by investigating the Spatiotemporal evaluations for different runs, the authors noticed that we could start seeing stop-and-go waves at medium densities when upstream propagation velocity is about $0.4 - 0.5$ m/s with critical density 3 ped/m.

2.3   Predicting Future Pedestrian Movement Characteristics

The recent advancements in Artificial Intelligence and its associated techniques have enabled researchers to develop advanced automated techniques for modeling and learning complex human motion behaviors. Different studies focus on using machine learning techniques in the PD field. Some of these studies proposed a prediction model to predict human future trajectories, while others focus on proposing prediction models to forecast movement quantities such as velocity used for human movement simulation. Along this line of research, several human trajectory prediction models have been proposed (Alahi et al., 2016; Hasan et al., 2018; Xue et al., 2017; Tordeux et al., 2019; Tkachuk et al., 2018; Ma, Lee, & Yuen, 2016). For instance, Alahi et. al. (Alahi et al., 2016) proposed Social - Long Short-term Memory (S-LSTM) human trajectory prediction model based on the architecture of the LSTM neural network. The proposed model has formed a basis for other LSTM-based human trajectory prediction models (P. Zhang, Ouyang, Zhang, Xue, & Zheng, 2019; Bisagno, Garau, Montagner, & Conci, 2019; Syed & Morris, 2019; Hasan et al., 2018). In this model, the prediction of each pedestrian future trajectory data depends on her/his previous positions and the neighbor's motion behavior around her/him. The authors used an LSTM network for each pedestrian to predict her/his future positions because each pedestrian has her/his motion pattern. Then, to capture other pedestrian interactions who are approximately spatially beside each other's (neighbors), they proposed a " Social-Pooling layer " that enabled sharing of the hidden state of each pedestrian's LSTM. The S-LSTM model was designed to predict only one possible future trajectory for each pedestrian who affected by surrounding neighbors. For this purpose, the model contains social pooling layers which collect the hidden states of the neighbors within a spatial distance of 64 coordinated before feeding it to the LSTM as input. A fixed hidden state dimension of 128 was used for all LSTMs. Additionally, a ReLU (Rectified Linear Units) activation function were used on the embedded hidden layers. For training and testing the model, the authors used publicly-available datasets namely ETH (Eidgenössische Technische Hochschule Zürich Walking Pedestrians dataset) [1], UCY (University of Cyprus crowd dataset) [2] and applied

---

[1]ETH dataset: `http://www.vision.ee.ethz.ch/en/datasets/`.

[2]UCY dataset: `https://graphics.cs.ucy.ac.cy/research/downloads/crowd-data`.

a cross-validation method to divide the data to training and testing datasets. Furthermore, for training, a learning rate of 0.003 and RMSprop optimizer was applied. The performance of the S-LSTM model compared against other state-of-the-art models: Linear model (Lin), Collision avoidance (LTA), Social force (SF), Iterative Gaussian Process (IGP), V-LSTM (S-LSTM model without social pooling), O-LSTM (V-LSTM model with occupancy map pooling). As stated by the authors, the Social-LSTM model was able to outperform state-of-the-art models in predicting various nonlinear behaviors arising from social interactions such as a group of pedestrians walking with each other. Another study was conducted by Xue et al. (Xue et al., 2017) to develop a trajectory prediction model; called the Bi-prediction model. This model addressed the issue of predicting the intended destination of pedestrians. The intended destination is important because pedestrians choose their routes based on this factor. The proposed two-stage human trajectory prediction model used a bidirectional LSTM architecture to predict multiple trajectories with different probabilities towards different destination regions in the scene. In this context, the model learns destinations in the scene and generates multiple trajectory predictions by classifying trajectories into a small number of " Route Classes " based on the source and the destination of the trajectory. The authors manually partitioned the region in the scene into different destination regions (candidates) based on the possible exit and entry for pedestrians. Then, the model predicted the destination regions and the probability of choosing each destination region for each pedestrian. After that, the model generated and predicted different sequences of trajectories concerning candidate route classes using one sub-LSTM that learns the movement behavior for each route class. The authors tested their Bi-prediction LSTM model using two public datasets: New York Grand Central [3] and Edinburgh Informatics Forum [4] and compared their model against Lin, SF, V-LSTM, S-LSTM, Attention-LSTM. In another model called MX-LSTM (Hasan et al., 2018) proposed by Hasan et al., the authors have added a new feature to the previous models to improve the human trajectory prediction which was the "direction of the head". In this context, we can predict the next position for any pedestrian by looking at his/her head direction (where he/she looks). So, using vislets; which is a short sequence of head pose estimation; the authors improved the human trajectory prediction. The proposed MX-LSTM

---

[3]New York Grand dataset: `http://www.ee.cuhk.edu.hk/~xgwang/grandcentral.html`.

[4]Edinburgh Informatics Forum dataset: `http://homepages.inf.ed.ac.uk/rbf/FORUMTRACKING/`.

model captured the interplay between tracklets (positional information) and vislets (head poses) to predict the future trajectory and also the future head poses. They manually partitioned the region in the scene into different destination regions (candidates) based on the possible exit and entry of pedestrians. The model was tested using public-domain datasets: UCY, Oxford Town Centre [5], and compared against Linear Trajectory Avoidance, SF, V-LSTM, S-LSTM models. On the other hand, other types of studies have focused on developing prediction models to predict movement quantities such as pedestrians' velocity. In the study of Tordeux et al. (Tordeux et al., 2019), the authors developed a Feedforward prediction model to predict the speed of pedestrians based on facility type. The authors focused on the type of buildings to predict various speeds since the behavior of pedestrians differs based on the type of facility where they move. The proposed model was tested and trained using two types of experiments: corridors, and bottleneck experiments. Four artificial neural networks were developed and tested with different inputs, hidden layers, and hidden neurons. The inputs of these models included relative positions to the 10 closest neighbors, relative velocities to the ten closest neighbors, and mean distance spacing to the ten closest neighbors. Also, eight different hidden layers and neurons fully connected with a Sigmoid activation function were tested. Cross-validation was applied to fit the models throughout training and testing steps. Besides, training the networks is performed using half of the data chosen randomly while testing with the remaining data. For training, the back-propagation method was used. The estimation results of the model were compared with the classical speed-based model (Parametric Weidmann Fitting Model). The results confirmed that the neural network models can distinguish and accurately predict the velocities of pedestrians in different facilities. For instance, for mixed data (corridor and bottleneck) the results were improved by 20% compared to the classical Weidmann fitting model (Bürgler & Lindenmann, 1994). Other studies predicted movement quantities and fed them back to the simulation system. Tkachuk et al. (Tkachuk et al., 2018) developed a system to simulate the behavior of pedestrians during the evacuation scenarios. The proposed system employed neural networks to predict how people act during evacuations. The system used the behavior of pedestrians and data from the evacuation experiments they performed to simulate emergency evacuation.

---

[5]Oxford Town Centre dataset: `https://megapixels.cc/datasets/oxford_town_centre/`.

To process those behaviors and their associated data, a FFNN model was used. Velocity and acceleration for each pedestrian that was obtained from the experiments were calculated mathematically at each step. Then the prediction model used the results to predict the horizontal and vertical velocities of each pedestrian on the next step. The neural network prediction model has one hidden layer and input layer that considered the surroundings of the subject pedestrian such as:

- Horizontal and vertical relative positions with other neighbors (1st, 2nd, 3erd, 4th, and 5th).

- Horizontal and vertical relative velocities with other neighbors (1st, 2nd, 3erd, 4th, and 5th).

- Distance from the left boundary, right boundary, and target line at the terminal.

- vertical and horizontal velocity of the subject pedestrian at the current time instant.

Python Tensorflow and Numpy libraries were used to create and train the neural network, and Java DL4j, Nd4j to make the visualization. These packages and libraries were all used then to simulate other evacuations. Finally, to verify the correctness of the trained neural network, they simulated the evacuation and compared how pedestrians moved on the video of the real experiment and how the pedestrians move in the simulation. The results have proved that this model provides higher accuracy in prediction by learning from existing real data rather than state-of-art models such as the Social Force model(Helbing & Molnar, 1995).

Inspired by the proposed neural networks based models, we aim in this study to build a prediction model to predict pedestrians' microscopic behavior characteristics, namely headway and velocity of pedestrians. Our proposed model will be distinguished by the fact that it exploits artificial neural networks to predict pedestrian movement behaviors in a closed corridor and single-file movement manner. We provide more details on our proposed prediction model in Chapter 6.

2.4 Summary

In this chapter, we have discussed several research works in the PD domain. We have classified the reviewed literature under two main categories. In the first category, we have presented and discussed the related work that focused on investigating PD characteristics in an aim to understand the main influential factors that contribute to the movement decisions made by humans while they move in both open and closed environments and paths. The context of research studies in this area was mainly concerned with conducting experiments that can assist precisely study human behavior under controlled conditions. In the second category, we have explored and discussed research works that have employed machine learning approaches to predict future human trajectory characteristics. The focus in this context is to develop applications that can learn from previous human movement trajectory data to predict and build future movement scenarios. We have highlighted the main strengths and limitations that are associated with existing experimental studies that pertain both categories. We have also provided our insights about the main factors that need further investigation, as well as those that we plan to predict using our proposed prediction model.

Chapter 3 — Empirical Study: Experiment, Data Collection, and Extraction

3.1 Introduction

The characteristics of pedestrian movement can be influenced and shaped by several factors. To study each of these factors in real-life scenarios, it is necessary to experimentally capture, acquire, analyze and study real-world human trajectory data. In this context, data collected from such experiments are quantified and used to calculate movement features such as pedestrians' velocity, density, and headway. In this work, experiments under laboratory conditions that comprised multiple runs were performed. The experiments were carried out in Palestine in an attempt to investigate the various movement characteristics of male and female pedestrians (males only, females only, and mixed-gender pedestrian groups) in a pre-defined set-up. To investigate pedestrians' movement characteristics, the movement of pedestrians in each experiment was filmed using a video camera, and then the trajectory data was extracted from these videos to calculate movement quantities.

This chapter is organized as follows: Section 3.2 introduces the single-file movement experiment set-up. In Section 3.3, we describe the steps of trajectory data extraction from video footage using PeTrack software (Boltes & Seyfried, 2013). Finally, Section 3.4 summarizes this chapter.

3.2 Set-up and Details of the Experiment

In this section, we present the single-file movement experiments that we have performed in Palestine with an aim of investigating gender-based movement characteristics. A series of controlled experiments were performed at the Arab American University in Palestine. The total number of participants was forty-seventh students (26 female, and 21 male) from different faculties and departments of the university. Their heights ranged from 152 cm to 184 cm and their

ages ranged from 18 to 23 years old. See Table 3.1 for a summary.

Table 3.1: Summary of participants' attributes.

Gender	Mean age	Mean height (m)	Number of participants (%)
Male	19	175.38	45%
Female	19	161.26	55%

As shown in Figure 3.1, an oval-shaped corridor which includes two semi-circles with an inner and outer radius of $r_1 = 1.45$ m and $r_2 = 2.05$ m respectively is used in this experiment. The width of the corridor $w = 0.6$ m prevents pedestrians from overtaking and forces a single-file movement. The length of the measurement section (straight part) is $l = 3.15$ m and the length of the whole corridor is $l_{corr} = 17.3$ m.
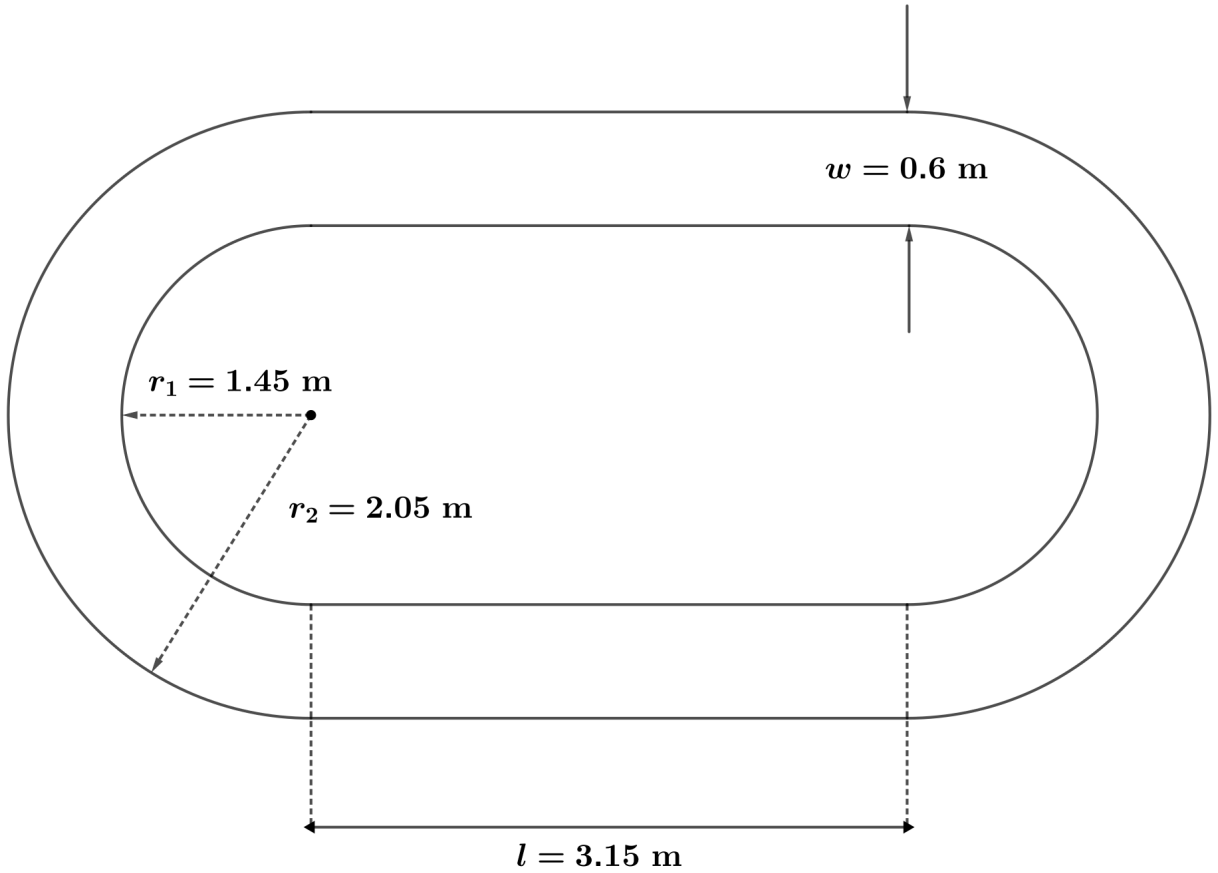
Figure 3.1: Sketch of the experimental set-up.

Two experimental set-ups were used: A and B with the same dimensions to perform the runs in parallel - one for female participants and the other for male participants - as shown in Figures 3.2 and 3.3. Besides, a separation board located in the middle area of the set-ups to limit the participants' view and to avoid overlap that can hinder the automatic extraction of the trajectories. To capture the pedestrians' motion inside the measurement section, two different cameras with settings: 25 FPS, 1600 ISO, 5.6 F-stop, 125 shutter speed, and 1280×720 resolution were used. The two cameras were set at a side view along the perpendicular bisector of the measurement section with a distance of 3.23 m and 3.44 m, and height from the floor of 0.86 m and 0.95 m respectively.

Figure 3.2: Snapshot of female run with $N = 14$.
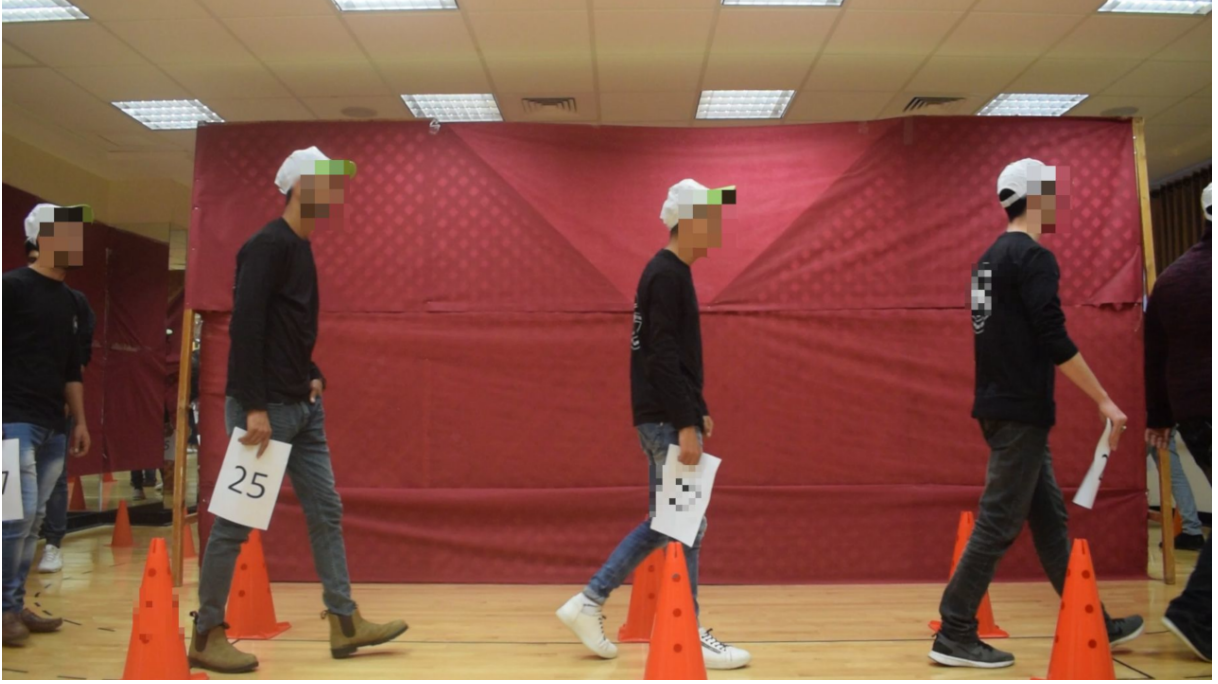
Figure 3.3: Snapshot of male run with $N = 14$.

Figure 3.4: Snapshot of a mixed run with $N = 14$.

The experiments focused on three gender-based compositions: female group, male group, and a mixed group (females with males). For each gender group, different runs were performed and repeated. In each run, we increased the number of pedestrians until we reached the critical

density or number of pedestrians available for the experiments. For female and male experiments we used the maximum available volunteers $N = 20$. For the mixed experiment, we reached a critical value $N = 38$ with a global density of $\rho = 2.19$ m^{-1} when the pedestrians stop walking and could barely move. Therefore, we had to reduce the number of pedestrians to $N = 30$, where the participants could start walking again.

Different groups of pedestrians were involved in each run to avoid bias that may happen if we extracted the data for the same group of pedestrians. Before the runs, the pedestrians were distributed uniformly along the corridor and instructed to move normally without overtaking for two to three cycles along the corridor; to increase trajectory data available for measurements . As shown in Table 3.2 three different types of runs were performed:

1. UF: Unidirectional flow female experiments. See Figure 3.2.

2. UM: Unidirectional flow male experiments. See Figure 3.3.

3. UX: Unidirectional flow mixed experiments (females and males together). The participants were positioned in an alternative manner depending on their gender (male-female-male-female- $\cdots$). See Figure 3.4.

Table 3.2: Details of gender-based experiments performed in Palestine.

| Index | Name | Repetition | Number of participants | | Global density $\rho\,(\mathrm{m}^{-1})$ |
			Female	Male	
01	UF_1	1	1	-	-
02	UM_1	1	-	1	-
03	UF_14	3	14	-	0.81
04	UM_14	3	-	14	0.81
05	UX_14	4	7	7	0.81
06	UF_20	3	20	-	1.16
07	UM_20	3	-	20	1.16
08	UX_20	4	10	10	1.16
09	UX_24	2	12	12	1.38
10	UX_30	2	15	15	1.73

At the first two runs, UF_1 and UM_1, seven pedestrians moved inside the corridor alone one after the other to calculate the average free-flow speed for males and females. In other runs, we gradually increased the number of pedestrians to realize different densities.

3.3 Data Collection and Extraction

The trajectories for each pedestrian at different time instances were automatically extracted from the captured video footage using PeTrack software (Boltes & Seyfried, 2013). Twenty-six videos from the experiments manipulated by multiple processing pipelines in the software: calibration, recognition, tracking, and analysis to extract precise position data. Firstly, the lens distortion and perspective views were corrected automatically through the calibration step using the captured chessboard pattern. After that, the 2-D coordinate system determined as precisely as possible starting from the beginning of the measurement section to the end. Then, to enable

PeTrack to recognize the pedestrians's, we detected the positions of pedestrians' heads in video recordings manually and then PeTrack automatically tracks them. Figure 3.5 shows a snapshot captured from PeTrack with the 4 main Tabs: calibration, recognition, tracking, and analysis. These Tabs correspond to the steps of the processing pipeline. For more information about PeTrack, please refer to (Boltes & Seyfried, 2013).
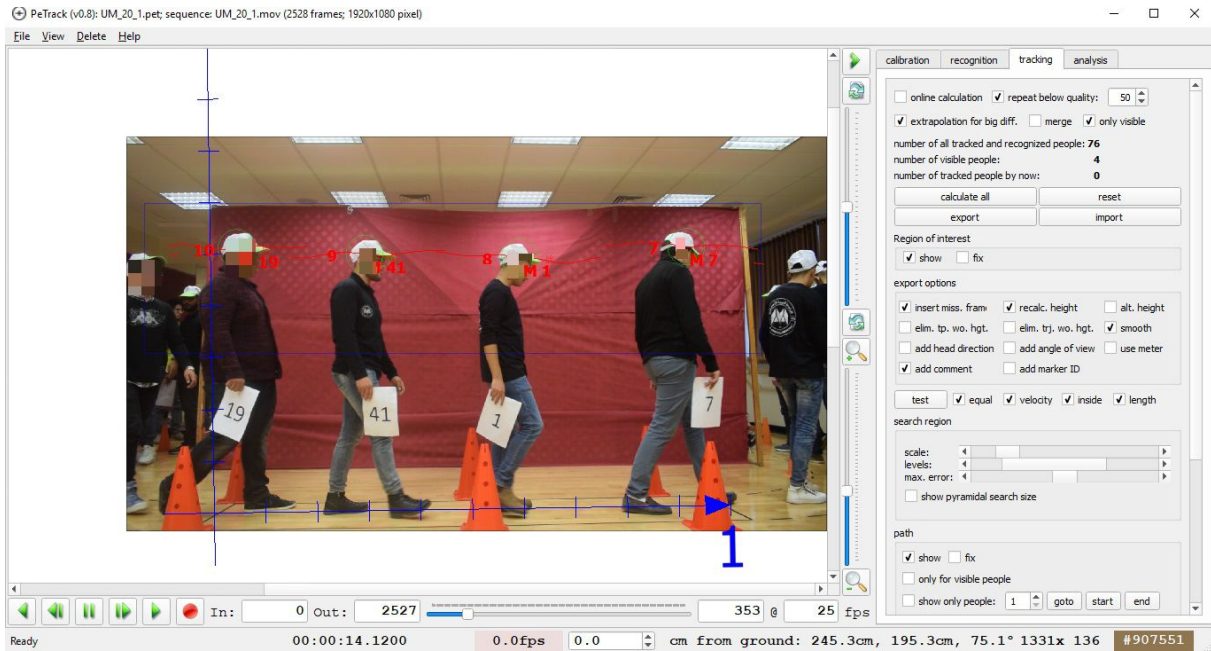
Figure 3.5: Snapshot of PeTrack during the extraction of trajectories.

The result of PeTrack software is a plain text files. Figure 3.6 shows a snapshot of an example file which contains the Personal information - pedestrian ID, and comment that contains pedestrians' gender with the paper sheet number- and frame ID (FR), Pedestrian ID (ID), x coordinates (X), y coordinates (Y), z coordinate (Z, we ignore it in 1-D scenarios), gender (comment, F or M) information.

```
UF_1.txt - Notepad
File  Edit  Format  View  Help
#description: experiment
#framerate: 25
#geometry: geometry.xml
#ID: the agent ID
#FR: the current frame
#X,Y,Z: the agents coordinates (in metres)
# personal information:
# ID| Comment
#  1 F 2
#  2 F 2
#  3 F 4
#  4 F 4
#  5 F 6
#  6 F 6
#  7 F 8
#  8 F 8
#  9 F 10
# 10 F 10
# 11 F 12
# 12 F 12
# 13 F 14
# 14 F 14
#ID      FR      X       Y       Z
1        0       0.2572  1.5620  0.0000
1        1       0.2795  1.5636  0.0000
1        2       0.3028  1.5625  0.0000
1        3       0.3266  1.5597  0.0000
1        4       0.3517  1.5587  0.0000
1        5       0.3751  1.5509  0.0000
1        6       0.4017  1.5512  0.0000
1        7       0.4252  1.5469  0.0000
1        8       0.4500  1.5471  0.0000
1        9       0.4732  1.5499  0.0000
1        10      0.4947  1.5514  0.0000
1        11      0.5139  1.5541  0.0000
1        12      0.5287  1.5540  0.0000
1        13      0.5452  1.5561  0.0000
1        14      0.5563  1.5563  0.0000
1        15      0.5659  1.5570  0.0000
1        16      0.5767  1.5590  0.0000
1        17      0.5866  1.5563  0.0000
1        18      0.5960  1.5582  0.0000
```

Figure 3.6: Snapshot of PeTrack-trajectory file for run $N = 1$.

3.4   Summary

In this chapter, we described the single-file movement experiments performed in Palestine to investigate pedestrians' dynamic characteristics. Accordingly, ten runs with different gender compositions and number of pedestrians were conducted and the movements of pedestrians were filmed using video cameras from the side view. Then, the videos were used for pedestrian trajectory data extraction using PeTrack software. The result of this step were plain text files that contained the trajectory data, which will be used to calculate movement quantities as we present in Chapter 4.

Chapter 4 — Movement Quantities Measurement Methods

4.1   Introduction

In this chapter, we present the measurement methods that we have applied to calculate the movement quantities (density, velocity, and headway). Two types of measurement methods were used to calculate pedestrians' velocity and density. One of the measurement methods is based on Voronoi diagrams (J. Zhang et al., 2014) and is used to calculate the movement basic quantities - individual mean velocity and density - with high accuracy and fewer fluctuations in comparison with other methods. Another method is the Classical method described in (Seyfried et al., 2005) which we used to measure the average velocity and density of pedestrians during different time instances.

The movement quantities of the experiments were calculated in the steady-state phase solely. As shown in Figure 4.1, the PD experiments were divided into three phases: start phase, steady-state phase, and end phase. The start phase indicates when pedestrians start moving throughout the corridor. At the beginning of their walking, the velocity is in a transient phase. After some relaxation time, we reach the steady-state phase, where the velocity fluctuations start to decrease. In the end phase, the velocity starts to increase in some runs when we opened the corridor to let them leave (for other runs we did not record the opening of the corridor).
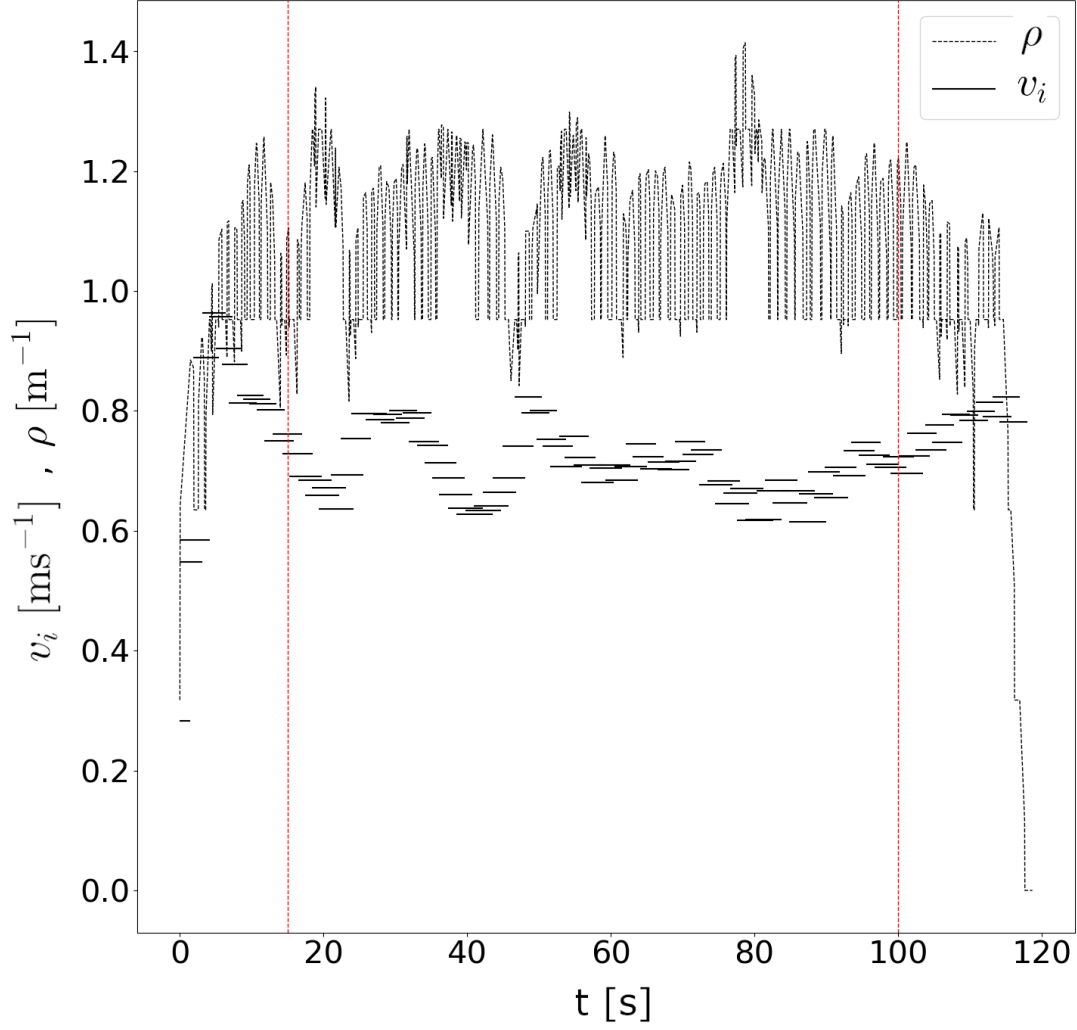
Figure 4.1: Time development of Classical density ρ and classical velocity v_i for female run $N = 20$. The two red lines indicate the steady-state limits. The length of the horizontal lines of v_i indicates the pedestrian time interval is inside the measurement section.

In this chapter, the FD (density-velocity relation) measurement methods are presented in section 4.2. While in section 4.3 the methods used to calculate headway are described. Finally, in section 4.4 we summarize the chapter.

4.2 Fundamental Diagram (Density-velocity Relation)

For the Voronoi method, the Voronoi space d_i of a pedestrian i is determined by the sum of half distances between the subject pedestrian and her/his neighbors. In other words, Voronoi space is the distance between the middle point of the predecessor $i+1$ pedestrian headway, and the middle point of the successor $i-1$ pedestrian headway as shown in Figure 4.2.
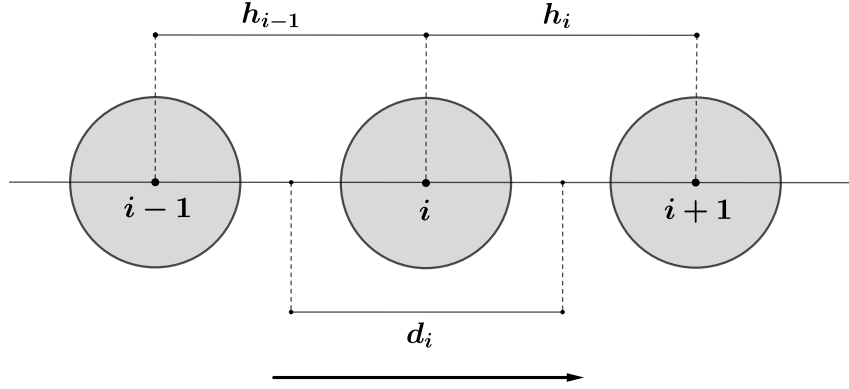
Figure 4.2: Illustration of a 1-D path indicates the distance headway of pedestrians i and $i-1$, and the Voronoi space d_i of pedestrian i. The walking direction of pedestrians is from left to right.

Therefore, the Voronoi individual mean density of pedestrian i at time t is defined as:

$$\rho_i(t) = \frac{1}{d_i(t)}, \tag{4.1}$$

$$d_i(t) = \frac{x_i(t) - x_{i-1}(t)}{2} + \frac{x_{i+1}(t) - x_i(t)}{2}, \tag{4.2}$$

where:

- $d_i(t)$ is the Voronoi space of pedestrian i at time t.

- $x_i(t)$ is the position of pedestrian i at time t.

During the experiment, we have a different number of pedestrians inside each video frame (different number of pedestrians inside the measurement area at each time instance). So, we need to consider all cases that may happen during our density calculations:

1. In the free-flow speed experiments the density is always zero. Because we have only one pedestrian inside the measurement section.

2. For higher density experiments; $N = 14, 20, 24, 30$; we have one pedestrian inside the measurement section or a pedestrian followed by one person without a predecessor, or a pedestrian preceded by a pedestrian without a successor, we ignored these cases.

3. In case we have a pedestrian preceded by a pedestrian and followed by another pedestrian. Then, equation 4.3 is used to calculate the individual mean density.

Moreover, the individual mean velocity of pedestrian i at time t calculated by the following equation:

$$v_i(t) = \frac{x_i(t + \Delta t/2) - x_i(t - \Delta t/2)}{\Delta t}. \tag{4.3}$$

Where $\Delta t = 0.4$ sec. (10 frames) which is a short time interval around t . Here, there are also different cases for velocity calculations:

1. When there is a pedestrian moving backwards (i.e. numerator is negative), in this case, the velocity is zero.

2. In case a pedestrian has a position in time Δt before, and also after the current time frame, then we use equation 4.3 to measure the velocity.

3. In case a pedestrian has only a position before Δt time frames, then the Δt equal to the pedestrian's exit frame.

4. In case a pedestrian has only a position after the Δt frames, then the Δt equal to the pedestrian's entrance frame.

Another measurement method is the Classical method described in (Seyfried et al., 2005). In this method, entrance and exit times are used to calculate the mean velocity of each pedestrian inside the measurement section using the classical definition:

$$v_i = \frac{x_i^{\text{out}} - x_i^{\text{in}}}{t_i^{\text{out}} - t_i^{\text{in}}}, \tag{4.4}$$

where:

- t_i^{out} is the exit time of pedestrian i from the measurement section.

- t_i^{in} is the entrance time of pedestrian i to the measurement section.

- v_i is the mean velocity of pedestrian i inside the measurement section during her/his time interval $[t_{in}, t_{out}]$.

- x_i^{out} is the location of pedestrian i when she/he leaves the measurement section.

- x_i^{in} is the location of pedestrian i when she/he enters the measurement section.

Because of the small number of pedestrians N involved inside the measurement section during each time step, the fraction $\Theta_i(t)$ between pedestrian i and pedestrian $i+1$ is used to calculate the mean density $\rho(t)$ during time t as:

$$\rho(t) = \frac{\sum_{i=1}^{N} \Theta_i(t)}{l_m}, \tag{4.5}$$

and

$$\Theta_i(t) = \begin{cases} \frac{t - t_i^{in}}{t_{i+1}^{in} - t_i^{in}} & : t \in [t_i^{in}, t_{i+1}^{in}], \\ 1 & : t \in [t_{i+1}^{in}, t_i^{out}], \\ \frac{t_{i+1}^{out} - t}{t_{i+1}^{out} - t_i^{out}} & : t \in [t_i^{out}, t_{i+1}^{out}], \\ 0 & : \text{Otherwise.} \end{cases} \tag{4.6}$$

where:

- l_m is the length of the measurement section (3.14 m).

- t_i^{in} is the entrance time of pedestrian i inside the measurement section.

- t_i^{out} is the exit time of pedestrian i outside the measurement section.

We should mention that for plotting the FD (velocity-density relation) we calculate the individual mean density ρ_i of pedestrian i which is the average values of $\rho(t)$ during her/his time-slice inside the measurement area. Also, the Classical method used in this research because we want to compare the results of the experiment with German and Indian results which were calculated using this method.

4.3 Headway

In general, when pedestrians walk, they keep a specific distance from their neighbors to move forward " Headway ". The headway is the distance between the subject pedestrian head and her/his predecessor's head as presented in Figure 4.2 previously. To measure the headway $h_i(t)$ of pedestrian i inside the measurement section at time t using the position data of pedestrians, the following formula is used:

$$h_i(t) = x_{i-1}(t) - x_i(t), \qquad (4.7)$$

Where:

- $x_{i-1}(t)$ is the x position of predecessor pedestrian $i-1$ at time t.

- $x_i(t)$ is the x position of subject pedestrian i at time t.

and to measure the headway using the density data available for Germany and Indian cultures, we use the below formula:

$$h_i = \frac{1}{\rho(t)}, \qquad (4.8)$$

where:

- $\rho(t)$ is the mean density at time t during pedestrian i time interval inside the measurement section.

4.4 Summary

This chapter aimed to present the measurement methods used to calculate the movement quantities using the pedestrians' trajectory data. In this research work, the Voronoi and Classical methods have been used to calculate the velocity and density of pedestrians. Also, for measuring pedestrian headways, we have utilized two types of measurement methods depending on the data available for calculations.

Chapter 5 — Comparative Analysis and Experimental Results

5.1 Introduction

As mentioned in the previous chapters, the factors that influence pedestrians' movement are diverse. Accordingly, studying these factors is crucial for real-life applications. In this chapter, the movement quantities of interest are represented and compared considering different factors including gender, culture, and age. Thus, the experimental results are divided into three parts based on the composition of pedestrians.

Section 5.2 discusses the gender-based FD (density-velocity relation), density-headway relation, and the velocity-headway relation for experiments conducted in Palestine. In Section 5.3, the cultural differences between Palestine, Germany, and India are analyzed based on the FDs (density-velocity relation), and velocity-headway relation. In Section 5.4, we present and compare the FDs and velocity-headway relations of different age groups from Palestine, and China.

5.2 Comparison Based on Gender Factor

Male and female participants have different psychological and physiological differences such as body size and behavioral reactions. To discover if the gender variations impact the movement characteristics of different gender compositions, a comparison between UX, UM, and UF experiments was conducted by comparing the FDs (density-velocity), velocity-headway, and density-headway relations.

5.2.1 Fundamental Diagram (Density-velocity Relation)

(a) FD (density-velocity) relation.

(b) FD (density-velocity) error bars.
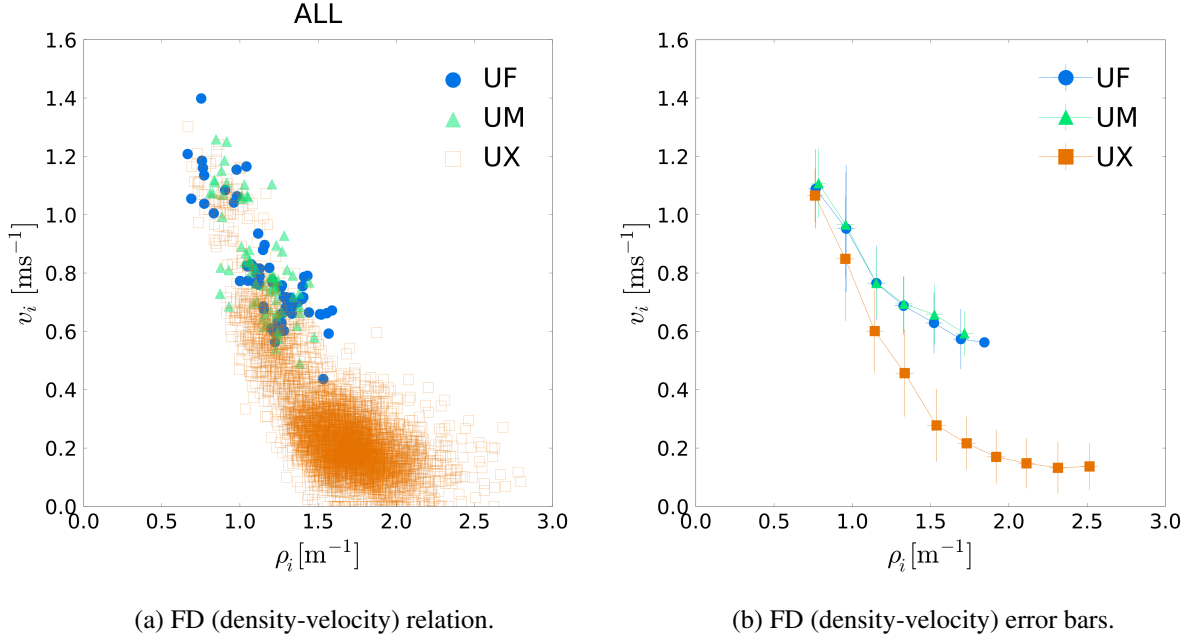
Figure 5.1: **Left:** The relation between FDs (density-velocity) of different gender groups: UF, UM, and UX. **Right:** The error bars of velocities of different density ranges, and bins are the mean velocity of each density range.

As depicted in Figure 5.1, UF experiments with $N = 14, \, 20$ pedestrians, UM experiments with $N = 14, \, 20$ pedestrians, and UX experiments with $N = 14, \, 20, \, 24, \, 30$ pedestrians were compared. By visually inspecting Figure 5.1 we observe the following: First, a typical negative correlation between the density of pedestrians and the velocity is observed. When the number of pedestrians inside the corridor increases, the velocity decreases, and the pedestrians start to walk slowly. Second, for different density groups, females and males walk approximately with similar velocities. For example, the mean velocities of females and males when the mean density equal to 1.5 m^{-1} are 0.62 ± 0.1 ms^{-1} and 0.65 ± 0.01 ms^{-1} respectively. Moreover, when the mean density is 1.7 m^{-1}, female participants walk with a mean velocity equal to 0.57 ± 0.1 ms^{-1} and the males walk with mean velocity of 0.59 ± 0.07 ms^{-1}. Another observation is that the velocity of male and female pedestrians changes significantly if they walk in

a mixed configuration, especially when the density is higher than 0.8 m^{-1}. For instance, the mean velocity of pedestrians walking in a mixed way for density 1.5 m^{-1} is $0.27 \pm 0.12 \text{ ms}^{-1}$.

The velocities of females and males at different densities are approximately similar as shown in Figure 5.1. However, their velocity changes significantly if they walk in a mixed group. Both males and females reduce their velocity when they walk in a mixed group as shown in Figure 5.2. The change of the females' mean velocity when the density equals to 1.5 m^{-1} is $1.28 \pm 0.12 \text{ ms}^{-1}$, and for males is $0.26 \pm 0.12 \text{ ms}^{-1}$. These results explain that Palestinian males and females tend to reduce their velocity when they walk in a mixed manner.

In conclusion, there is no noticeable difference in the way the males and females walk in homogeneous groups. While, the differences exist if they walk together in a heterogeneous group. The reason for these differences is the social conventions and common-sense rules in Palestine, where the males and females prefer to have a long personal space when they move beside each others.
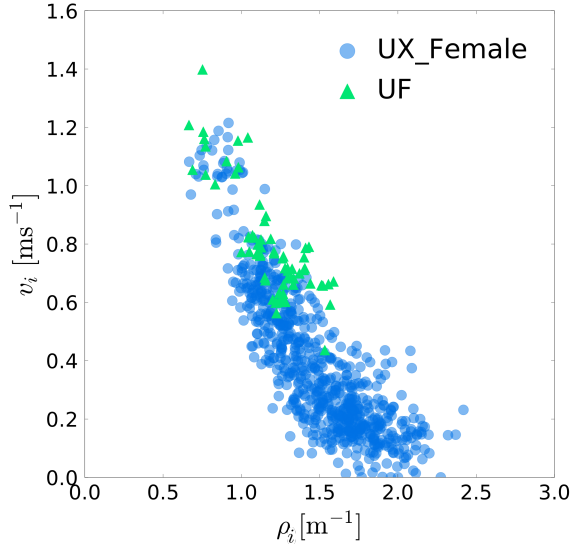
(a) Female on UX and UF.
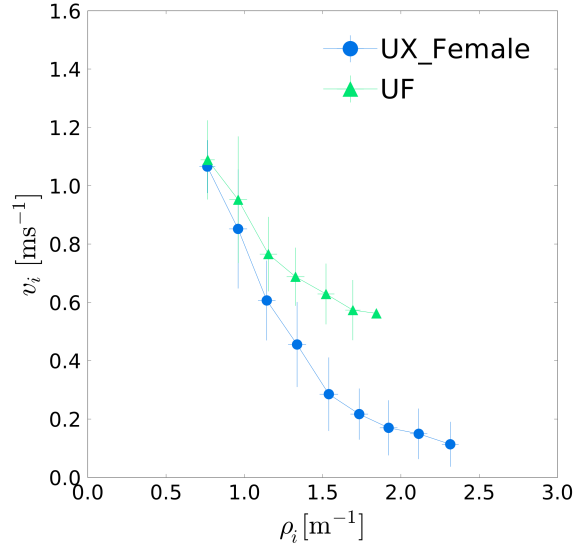
(b) Density-velocity error bars.
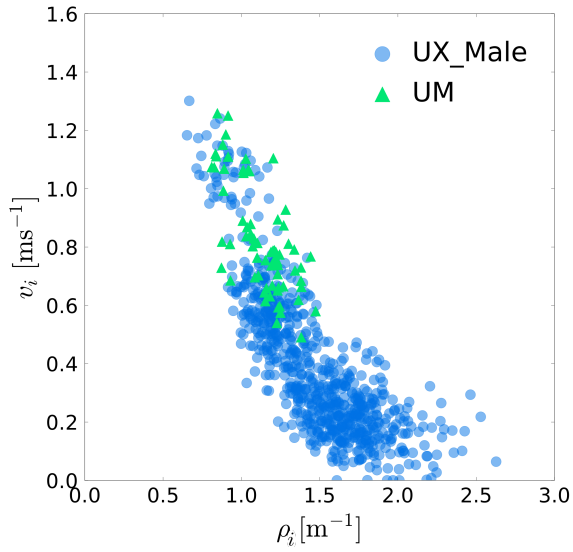
(c) Male on UX and UM.
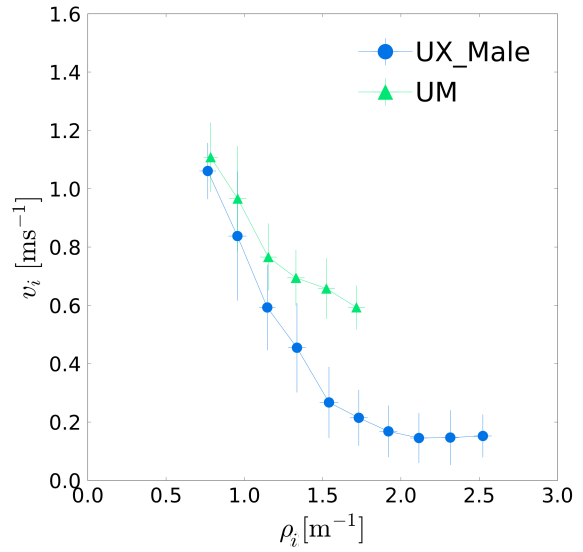
(d) Density-velocity error bars.

Figure 5.2: **Up:** Comparison between the FD (density-velocity) relation of females inside the UX experiments and inside UF experiments for different densities. **Down:** Comparison between the FD (density-velocity) relation of male inside UX experiments and inside UM experiments for different densities.

5.2.2 Density-headway and Velocity-headway Relations

Another movement characteristic studied in this section is the headway 4.7. As shown in Figure 5.3 the pedestrians' headway decreases with the increase of pedestrians number inside the corridor for all gender groups with the same quantity. For example, for density 0.7 m^{-1} the females and males have a headway of 1.3 ± 0.3 m and 1.25 ± 0.2 m respectively. Additionally, for different densities, we get different headway values due to the reduction of space inside the measurement section, but the same for similar densities of different gender groups.

(a) Density-headway relation.

(b) Density-headway error bars.

Figure 5.3: **Left:** The relation between density-headway of different gender compositions. **Right:** The error bars of the relation.

To investigate whether the females keep a larger headway than males (or not) during their walk in UX experiments, the distance headway between each pedestrian and her/his predecessor and the distance between the pedestrian and her/his successor were measured. From Figure 5.3 it can be noticed that there is no obvious difference between the headway of different densities in UM and UF experiments. For density 0.7 m^{-1} females keep a distance of 1.29 ± 0.26 m while walking, and males keep a distance of 1.3 ± 0.28 m respectively. That means both males and females keep the same distances when they move inside the corridor in a mixed group.

Furthermore, by comparing the distance headway of UM experiments with the UX experiments we can notice that the headway is approximately the same for similar densities. That means if the males walk with other males they will keep the same distance as if they walk with other females for the same density and vice versa. See Figures 5.3 and 5.4.

(a) Headway-frequency UF   (b) Headway-frequency UM   (c) Headway-frequency UX
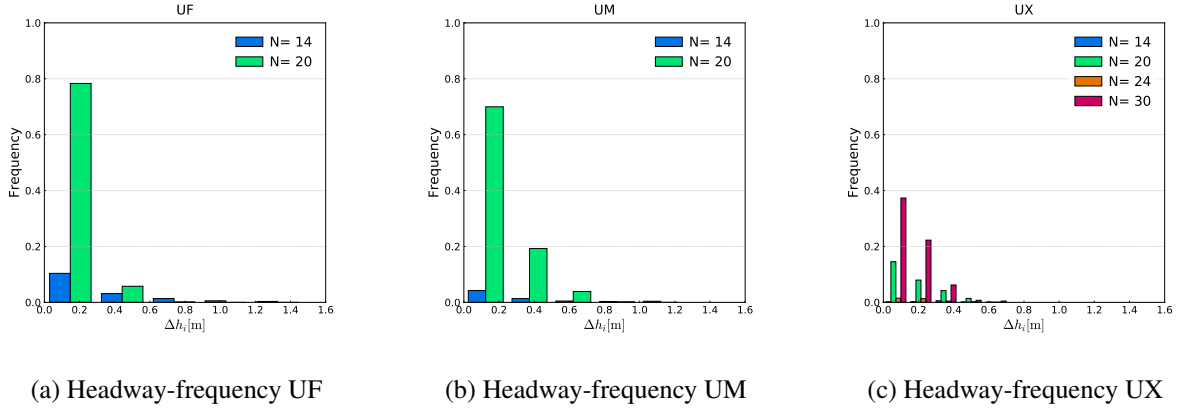
Figure 5.4: Histograms show the density-headway differences between the headway of subject pedestrian and the headway of follower pedestrian for different gender compositions.

For velocity-headway relation, the results showed that the speed of pedestrians varies depending on gender composition. The pedestrians in UX experiments walk slower than pedestrians in UM and UF experiments with the same headway as showed in Figure 5.5. For instance, to reach velocity 0.7 ms^{-1} a headway distance of 0.79 ± 0.1 m for females on UF experiments is required, while on UX experiments headway distance of 0.9 ± 0.13 m is required. Similarly, males velocity 0.7 ms^{-1} achieved with a headway of 0.77 ± 0.14 m in UM experiments, and 0.86 ± 0.14 m in UX experiments. Therefore, it is observed that more distance required in UX experiments to achieve the same velocity of UM and UF for the same density.
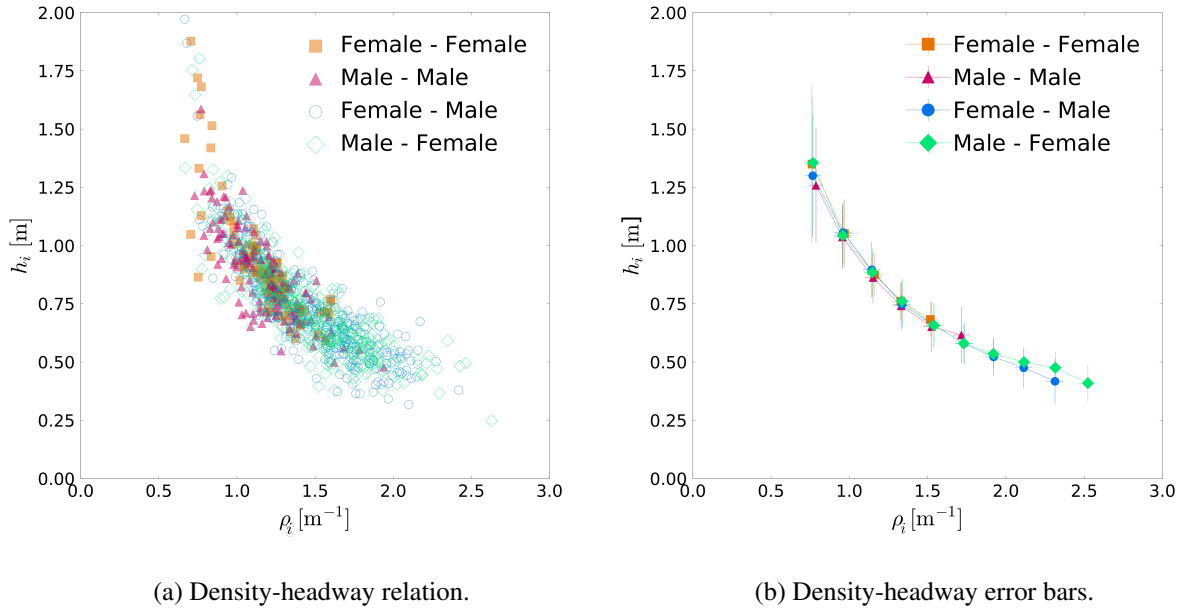
(a) Velocity-headway relation.

(b) Velocity-headway error bars.
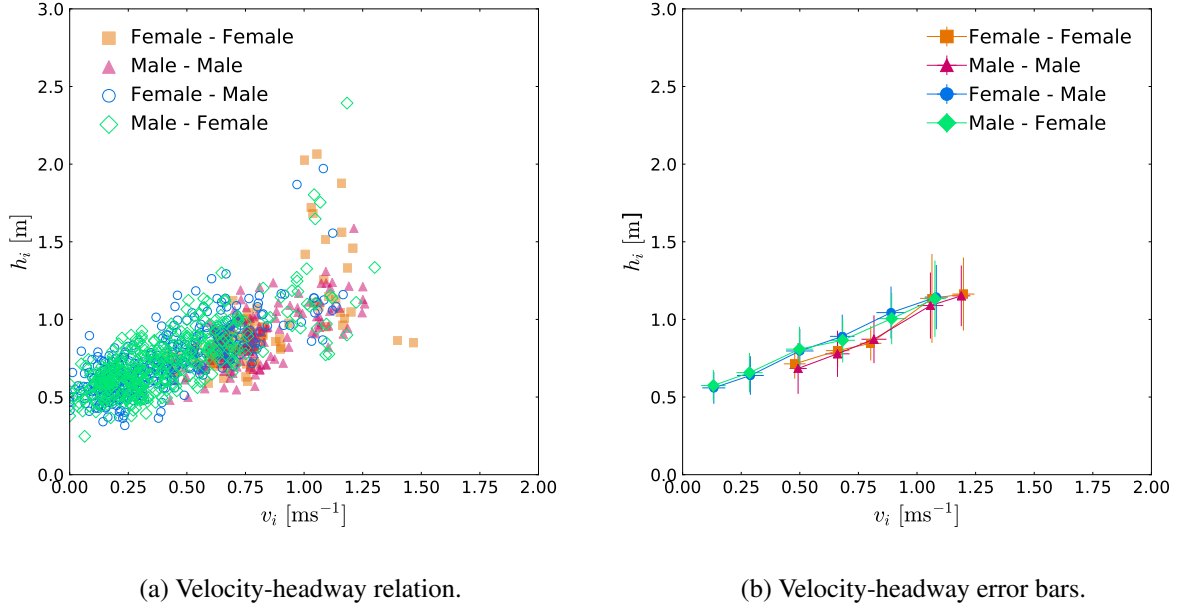
Figure 5.5: **Left:** The relation between velocity-headway of different gender compositions. **Right:** The error bars of the relation

5.3   Comparison Based on Social Conventions Factor

One of the factors that influence the FDs is the social conventions factor (Chattaraj et al., 2009). In this section, a comparison between Palestine experiments ($N = 14,\ 20$) and other single-file movement experiments performed in Germany (Seyfried et al., 2005) ($N = 15,\ 20$), and in India (Chattaraj et al., 2009) ($N = 15,\ 20$) was conducted. The measured density and velocity of the German and Indian experiments are publicly available online in the Pedestrian dynamics data archive [1], and to calculate the density and velocity for Palestine experiments we used the same measurement method described in (Seyfried et al., 2005).

To scrutinize the impact of the culture factor on the pedestrian dynamics, we tried to keep other factors comparably unchanged. Thus, we compared UM experiments (India, and Palestine) with approximately the same densities, and compared UX experiments (Germany and Palestine) with approximately the same densities as well, since the dynamics of pedestrians change depending on the gender composition within a group (see results of Section 5.2).

---

[1]Pedestrian dynamics data archive: `http://ped.fz-juelich.de/da/2005singleFile`.

5.3.1 Fundamental Diagram (Density-velocity Relation)

We should notice that in Palestine UX experiments the pedestrians are arranged in an orderly manner and the number of males in each run is equal to the number of females (balanced). But in German UX experiments, the pedestrians are ordered randomly and the number of males is not equal to the number of males in each run (unbalanced). In Figure 5.6 the FD (density-velocity relation) of Palestinian UX and German UX are presented. We can observe that Germans walk slower than Palestinians in UX experiments in low densities. For instance, when the density is equal to 0.7 m^{-1} Palestinians walk with velocity 0.99 ± 0.1 ms^{-1}, while Germans walk with a velocity of 0.92 ± 0.01 ms^{-1}.

(a) Density-velocity relation.

(b) Density-velocity error bars.
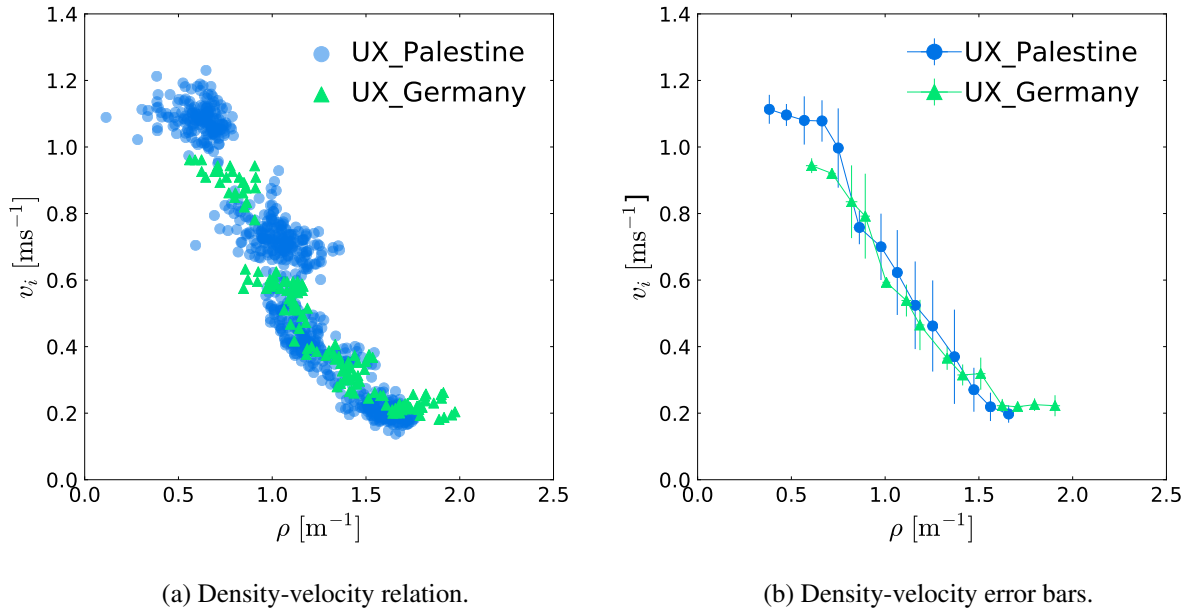
Figure 5.6: **Left:** The relation between the FD (density-velocity relation) of German and Palestinian UX experiments with approximately with the same densities. **Right:** The error bar of the relation.

Moreover, for Indian UM and Palestinian UM experiments as shown in Figure 5.7 we have observed that the Palestinian pedestrians' density in each run is lower than the density of Indian pedestrians, especially in run $N = 14$. This means that compared to Palestinians, Indian males walk beside each other with a smaller comfort zone. Another observation is that the velocity of

Palestinians affected highly by the increase of density rather than the Indians, which we can see in shrinking space between the different runs.

(a) Density-velocity relation.

(b) Density-velocity error bar.
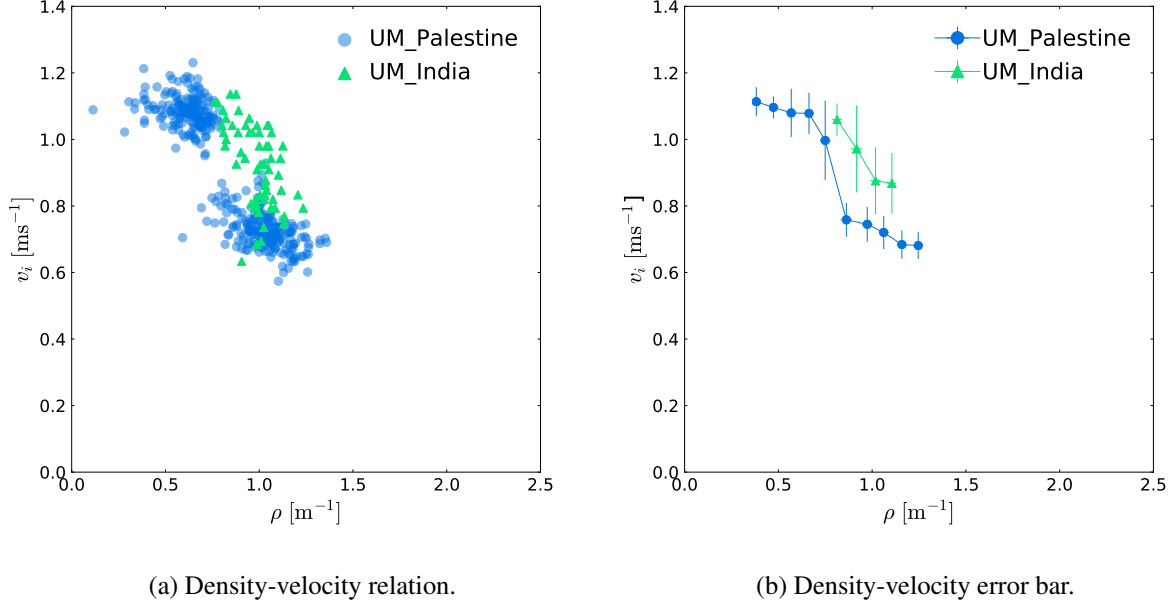
Figure 5.7: **Left:** FD (density-velocity relation) between Indian UM and Palestinian UM in single-file movement experiments approximately with the same densities. **Right:** The error bar of the relation.

5.3.2 Velocity-headway Relation

In this section, the headway defined as the inverse of density (Equation 4.8) is studied. Figure 5.8 represents the relation between Palestinian UX and German UX, and Palestinian UM and Indian UM velocity-headway relation for several densities. We have noticed that Palestinian males keep more distance when they walk in corridors than Indian males who walk beside each others much more closely. Another observation is that German pedestrians keep longer distances than Palestinians in the UX runs in densities approximately between 0.6 m^{-1} and 0.9 m^{-1}. So, the velocity-headway relation results confirmed that the social convention factor has a significant impact on PDs.
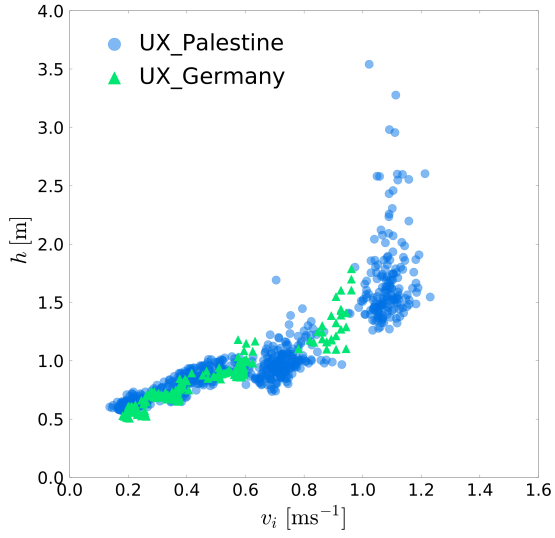
(a) Germany and Palestine.
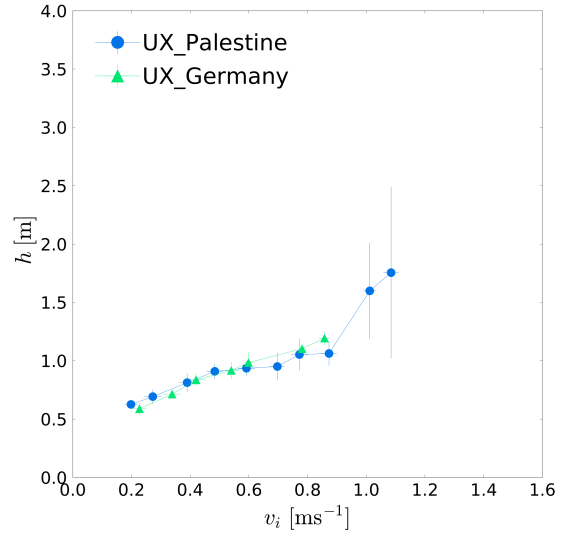
(b) Velocity-headway error bars.
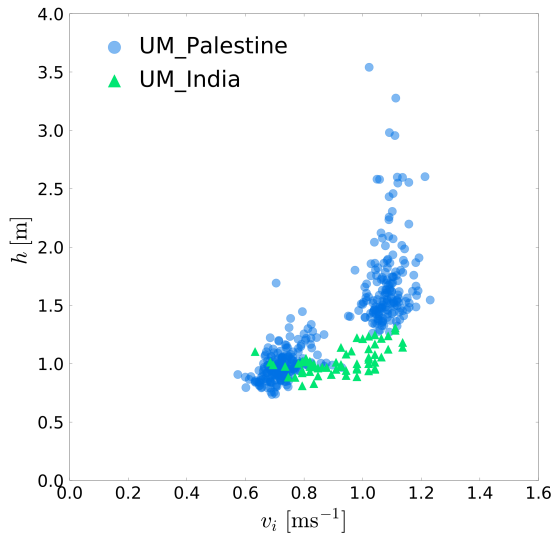
(c) India and Palestine.
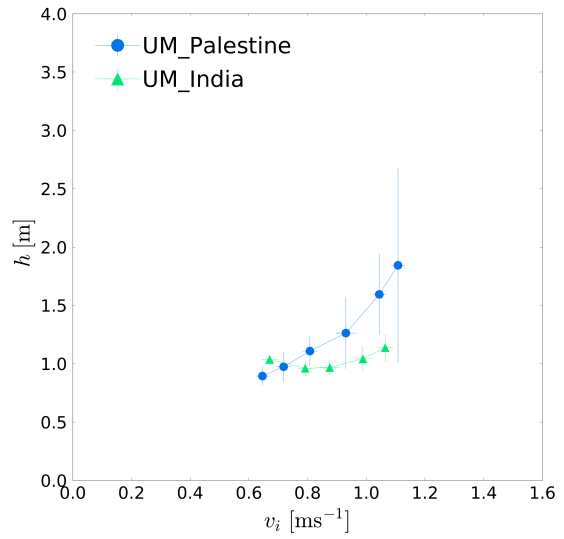
(d) Velocity-headway error bars.

Figure 5.8: **Up:** Velocity-headway relation of Germany UX and Palestine UX single-file movement experiments with approximately the same densities. **Down:** Velocity-headway relation of Indian UM and Palestinian UM single-file movement experiments approximately with the same densities.

5.4   Comparison Based on Age Factor

In this section, the pedestrians' movement proprieties of different age groups were investigated. The movement quantities - FD (density-velocity relation), and velocity-headway relation - of Palestine UX experiments were compared against China single-file movement experiments (Cao et al., 2016) with approximately the same number of pedestrians in each run. In China experiments, there are two types of age-based experiments: young experiments with mean age equal to 17 (16-18 years old) and old experiments with mean age equal to 52 (45-73 years old). In age-based comparison, the Equations 4.1, 4.3, and 4.2 used to calculate the movement quantities: density, velocity, and headway respectively. The trajectory data of China experiments are publicly available in PD data archive [2].

5.4.1   Fundamental Diagram (Density-velocity Relation)

Considering the results of (Cao et al., 2018), we compared UX experiments of mean age 19 with China (old, young 17) UX experiments. Figure 5.9 shows that Palestinian young pedestrians walk slower than Chinese young pedestrians in UX experiments. It is no surprise that Palestinian young pedestrians walk faster than Chinese old pedestrians in low densities. However, old Chinese pedestrians walk faster than Palestinian young pedestrians when they walk in a mixed composition in high densities (density is more than 1.45 m^{-1}). We assumed that these differences originate by differences in culture and social conventions that define the accepted comfort zone between pedestrians. This result indicates that while the age factor impacts the movement of pedestrians, it is also governed by the culture factor if we compared different age groups from different cultures.

---

[2]China dataset: `http://ped.fz-juelich.de/da/2005singleFile`.

(a) Density-velocity relation.

(b) Density-velocity error bars.
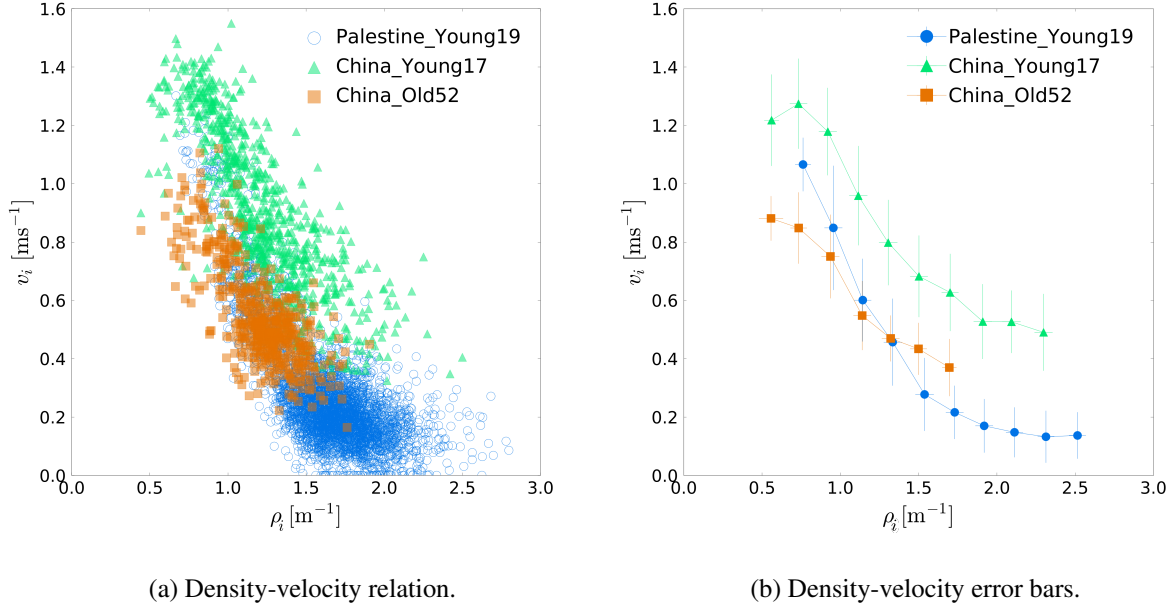
Figure 5.9: **Left:** FD (density-velocity relation) for three age groups: Palestinian young (average age of 19 years), China young (average age of 17 years), and China old (average age of 52 years). **Right:** Bars of binning the velocity-headway relation.

5.4.2 Velocity-headway Relation

Figure 5.10 represents the velocity-headway relation of the three age compositions. With the increase of velocity, Chinese young pedestrians walk with more available headway in comparison with Chinese old pedestrians and Palestinian young pedestrians. Besides, the Palestinian young and Chinese old velocities become close when the density equal to 1.3 m^{-1} and they walk with the same headway for velocity lower than 0.5 ms^{-1}. In addition, for velocities higher than 0.5 ms^{-1}, Palestinian young pedestrians walk with headway shorter than old Chinese. Based on the above comparison, it's confirmed that younger pedestrians walk faster with shorter headway than older pedestrians, and that depends on the culture difference.

(a) Velocity-headway relation.

(b) Velocity-headway error bar.
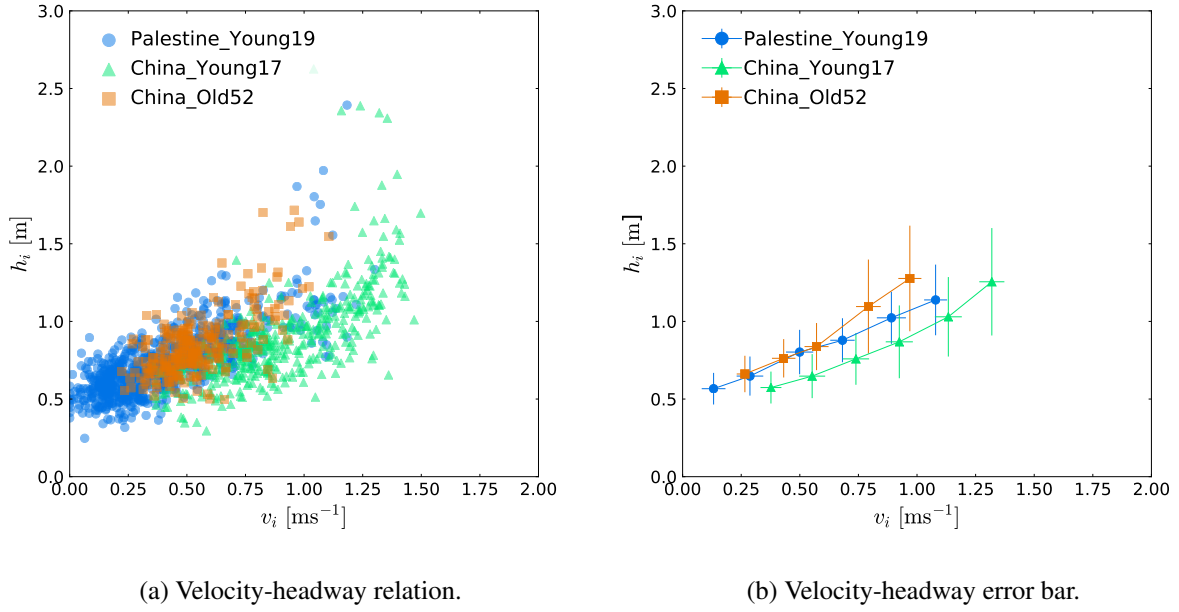
Figure 5.10: **Left:** Velocity-headway relation for different age groups: Palestinian young (average age of 19 years), China young (average age of 17 years), and China old (average age of 52 years). **Right:** Bars of binning the velocity-headway relation.

5.5 Hypothesis Testing (Kolmogorov-Smirnov Statistical Test)

Finally, for hypothesis testing of all comparison parts, the Kolmogorov-Smirnov statistical test (two-sample K-S test) (Simard & L'Ecuyer, 2011) was chosen because independent samples of data points were obtained from movement quantity's comparisons. The null hypothesis H_0 for each comparison case was defined. If the Kolmogorov-Smirnov value D-Statistic is greater than the D-Critical value of the expression:

$$D_\alpha = c(\alpha)\sqrt{\frac{n_1 + n_2}{n_1 \cdot n_2}}\,, \tag{5.1}$$

where:

- $c(\alpha)$ is the coefficient (0.05 level of significance).

- n_1 is the number of sample 1 data points.

- n_2 is the number of sample 2 data points.

then we reject the null hypothesis. Tables 5.1, 5.2, 5.3, 5.4, 5.5, and 5.6 summarize the results of the test for samples of reduced data in steady-state.

Table 5.1: Description of Density-velocity relation (gender) Kolmogorov-Smirnov statistical test results.

Density-velocity relation (gender)				
Sample 1	**Sample 2**	**D-Statistics**	D_α	**Reject/Accept H_0**
UM_14_20	UF_14_20	0.166	0.231	Accept
UM_14_20	UX_14_20	0.387	0.174	Reject
UF_14_20	UX_14_20	0.331	0.179	Reject
UM_14_20	UX_Male_14_20	0.389	0.186	Reject
UF_14_20	UX_Female_14_20	0.298	0.192	Reject

Table 5.2: Description of Velocity-headway relation (gender) Kolmogorov-Smirnov statistical test results.

Velocity-headway relation (gender)				
Sample 1	**Sample 2**	**D-Statistics**	D_α	**Reject/Accept H_0**
UF_Female-Female	UM_Male-Male	0.143	0.174	Accept
UX_Male-Female	UX_Female-Male	0.0403	0.100	Accept
Female-Male + Male-Female	Female-Female	0.434	0.139	Reject
Female-Male + Male-Female	Male-Male	0.358	0.126	Reject

Table 5.3: Description of Density-velocity relation (culture) Kolmogorov-Smirnov statistical test results.

Density-velocity relation (culture)				
Sample 1	**Sample 2**	**D-Statistics**	D_α	**Reject/Accept H_0**
UX_Palestine	UX_Germany	0.327	0.123	Reject
UM_Palestine	UM_India	0.365	0.187	Reject

Table 5.4: Description of Velocity-headway relation (culture) Kolmogorov-Smirnov statistical test results.

Velocity-headway relation (culture)				
Sample 1	**Sample 2**	**D-Statistics**	D_α	**Reject/Accept H_0**
UX_Palestine	UX_Germany	0.222	0.123	Reject
UM_Palestine	UM_India	0.456	0.187	Reject

Table 5.5: Description of Density-velocity relation (age) Kolmogorov-Smirnov statistical test results.

Density-velocity relation (age)				
Sample 1	**Sample 2**	**D-Statistics**	D_α	**Reject/Accept H_0**
Palestine_Young19	China_Young17	0.836	0.052	Reject
Palestine_Young19	China_Old52	0.720	0.064	Reject

Table 5.6: Description of Velocity-headway relation (age) Kolmogorov-Smirnov statistical test results.

Velocity-headway relation (age)				
Sample 1	**Sample 2**	**D-Statistics**	D_α	**Reject/Accept H_0**
Palestine_Young19	China_Young17	0.280	0.084	Reject
Palestine_Young19	China_Old52	0.306	0.100	Reject

5.6 Summary

In this chapter, we discussed the results of Palestine single-file movement experiments compared to other experiments: Germany, India, and China. The comparison in this research focused on three factors that influence the movement characteristics: gender, social conventions, and age. It is concluded that gender factor has no impact on the movement characteristics of pedestrians if they walk in a homogeneous group. In contrast, if the female and male pedestrians walk together, they will change their velocity and headway. Moreover, the results confirm that culture and age factors have a significant effect on pedestrian movement characteristics.

Chapter 6 — Movement Quantities Prediction Model

6.1 Introduction

In real-life scenarios, the dynamics of pedestrians are normally controlled by several social and behavioral factors. In Chapter 5, we conducted an intensive analysis to investigate the impact of different factors on pedestrian movement characteristics. In this chapter, the goal is to propose a prediction model to precisely forecast future velocities and headway distances for various pedestrian compositions and densities. To learn the PD patterns and recognize the relationship between pedestrian movement behavior variables, researchers exploit machine learning approaches to assist in identifying the influence of each factor on the one hand, and enable them to predict future pedestrian behaviors on the other. Different state-of-the-art models such as the Social-force model (SF) (Helbing & Molnar, 1995) and the parametric Weidmann fitting model (Bürgler & Lindenmann, 1994) described pedestrians' motion using formulas which make the movement of each pedestrian becomes too mechanical and not similar to the real pedestrian's motion. On the other hand, recent prediction models - using neural networks - have proved to be more effective in predicting movement quantities for different set-ups and densities. For instance, using FFNN, Tordeux and his colleagues were able to predict the velocity for a different type of facilities (Tordeux et al., 2019). In this chapter, we exploit the same prediction model to investigate and predict future velocity and headway data using the data that we have acquired using single-file movement experiments that were conducted in Palestine and China (Cao et al., 2016). Multi-layer Perceptron (MLP) Feedforward neural network is used to build our prediction model. Multiple training and testing groups were tested to accurately predict future motion details. Additionally, multiple factors, such as age, gender and velocity were incorporated in the prediction model in an attempt to investigate their impact on the produced results.

6.2 Experimental Evaluation of the Proposed Prediction Model

In this section, we discuss the steps that we have carried out in order to evaluate the quality of the proposed prediction model. In particular, two different datasets were used: Palestinian data from Palestine single-file movement experiments, and China single-file movement experiments - that we used previously for age factor comparison -. Our purpose in this context was to train, validate, and further test our prediction model using well-recognized, real-world and trusted pedestrian trajectory data. The Palestinian dataset contains pedestrians' gender information, in addition to the trajectories of each pedestrian that have been captured at different time frames. All pedestrians were with an average age of 19 years old. The data from three runs used: UM, UF, and UX groups. On the other hand, the China dataset contains two types of experiments: young experiments (mean age of 17 years old), and adults (mean age of 52 years old). The dynamically-calculated movements' quantities - density, velocity, and headway - and their associated pedestrian information were used as input features to the FFNN model.

We have experimentally tested five scenarios for the models: Scenario 1, Scenario 2, Scenario 3.1, Scenario 3.2, Scenario 4. The scenario details and datasets used in our model are described in Table 6.1. These datasets were divided into a training dataset to train our model, validation dataset to evaluate the model during each epoch, and testing dataset to test the model in making future predictions. We have followed this approach (Kuhn & Johnson, 2013) of dividing data to:

- Build a solid model that trained and tuned using the training data.

- Evaluate the model during each epoch using the validation data that are unseen by the model, to help us tune our model hyper-parameters.

- Further test the produced results using new data (testing dataset).

Each group in the datasets contained different records obtained from different density experiments. The training dataset contained runs with a variable number of pedestrians: $N = 14, 15, 16$, while the validation dataset included: $N = 20, 21$. The testing dataset contained: $N = 24, 25, 26, 30$.

Table 6.1: Empirical data of Palestine and China experiments divided into training, validation, and testing datasets for different scenarios.

Scenario	Dataset	Run name	Number of records
Scenario 1, 2, 3.1, 3.2	Training dataset	UF_14_1	8398
		UF_14_2	
		UF_14_3	
		UM_14_1	
		UM_14_2	
		UM_14_3	
		UX_14_1	
		UX_14_2	
		UX_14_3	
		UX_14_4	
Scenario 1, 2, 3.1, 3.2	Validation dataset	UF_20_1	3000
		UM_20_1	
		UX_20_1	
Scenario 1, 2	Testing dataset	UX_24_1	2000
		UX_30_1	
Scenario 3.1	Testing dataset	China_adults_16	2000
		China_adults_21	
		China_adults_26	
		China_adults_30	
Scenario 3.2	Testing dataset	China_students_15	2000
		China_students_20	
		China_students_25	
		China_students_30	
		UX_14_1	
Scenario 4	Training dataset		11245

Continued on next page

Table 6.1 Continued from previous page.

Scenario	Dataset	Run name	Number of records
		UX_14_2	
		UX_14_3	
		UX_14_4	
		China_adults_16	
		China_students_15	
Scenario 4	Validation dataset	UX_20_1	5011
		China_adults_21	
		China_students_20	
Scenario 4	Testing dataset	UX_24_1	3000
		UX_30_1	
		China_adults_26	
		China_adults_30	
		China_students_25	
		China_students_30	

6.3 Detailed Characteristics of the Proposed Prediction Model

Inspired by the works proposed in (Tordeux et al., 2019; Tkachuk et al., 2018; Ma et al., 2016; Das, Parida, & Katiyar, 2015; Tordeux, Chraibi, Seyfried, & Schadschneider, 2018), we proposed a Multi-layer Perceptron FFNN prediction model. It is important to point out that, unlike the previously cited literature where the authors focused on the relative position and mean space parameters to predict the velocity, we used a set of input features; as we further detail in the next sections; to predict the headway and velocity of each pedestrian using different densities. As such, different models have been built depending on the empirical data available. Each model contains three types of layers: an input layer, hidden layers, and an output layer. Also, each model contains different input features and a different number of hidden layers and hidden

neurons. In our problem domain, the dependent variable is headway and velocity, and other related independent variables are velocity, density, subject pedestrian gender, and predecessor pedestrian gender.

During the training process, we tuned the hyper-parameters - number of hidden layers, number of hidden neurons, activation function, optimizer, learning rate, regularization - to reach the robust model. For all models, we used Sigmoid activation function, Adam optimizer with a learning rate of $l_r = 0.003$, and the loss function " Mean-Square-Error " to calculate the error between predicted and real headway values. Keras library written in python was used to build the prediction models.

6.3.1 Input Layer

The input layer receives parameters that indicate the movement behavior of the pedestrian in the crowds. Each group of models contains different input features:

1. Density: it represents the space occupied by a person and the number of pedestrians inside the measurement section.

2. Properties of subject pedestrian:

    (a) Age.

    (b) Gender.

3. The velocity of the subject pedestrian (only in Scenario 1).

4. Properties of neighbors (predecessor):

    (a) Gender.

In each prediction model, different combinations of input features were applied to conduct a comparison between their results. We want to know which input features improve the predictions and have a strong relation with headway. The main number of input neurons (parameters) is different depending on the input features used for each model.

6.3.2 Hidden Layers

There is no unified approach to decide the number of hidden layers and neurons. Following rules-of-thumb, most commonly relied on Jeff Heaton (Heaton, 2008) approach " the optimal size of the hidden layer is usually between the size of the input and size of the output layers ". So, we tried different combinations of hidden layers and neurons (1), (2), (3), (3,2), (2,2), where (x) represent one hidden layer with x number of hidden neurons, and (x,y) represents two hidden layers with number x of hidden neuron in the first layer and y number of neurons in the second hidden layer. We used the same activation function for all layers.

6.3.3 Output Layer

The output layer in the proposed neural networks produces the value of prediction which is the velocity of pedestrians for scenario 1, and headway and velocity of pedestrians for scenarios 2, 3.1, 3.2.

6.3.4 Prediction Models

Several neural networks are trained by tuning their hyper-parameters to get an acceptable and high-performance model. The first step of building our model is preprocessing our datasets and dividing it into three datasets: training, validation, and testing. The data is normalized by scaling it between 0 and 1. Normalization is necessary to change the values of numeric columns in the dataset to a common scale, without distorting differences in the ranges of values. For our data, the normalization is required because input features have different ranges.

For our models, we used the Sigmoid activation function for each dense layer with initial weights and initial bias that are chosen randomly. Then, we configured the models with different parameters. Also, Adam optimizer is used with a learning rate of 0.003. The MSE cost function is described by the formula:

$$MSE = \frac{1}{n} \sum_{i=1}^{n} (Y_i - \hat{Y}_i)^2, \tag{6.1}$$

where:

- Y_i is the actual (real) velocity of the pedestrian.

- $\hat{Y}_i$ is the predicted velocity of the pedestrian.

- n is the number of observations (sample data points).

We aim to minimize the MSE to get a high-performance prediction model. Finally, the models were fitted using 100 epochs which was enough to see the progress of learning in most cases and a batch size that equals to 10. Back-propagation was then used to update the weight values during the training process.

6.4 Prediction Models Results

6.4.1 Scenario 1

The results of the prediction models indicate that the models contain density as input features outperform other models without density (such as NN2, NN4). Also, in NN1 one hidden layer with one neuron is enough to predict the headway with low MSE. Other networks such as NN3, NN5, NN6 one layer with 1,2, or 3 neurons give the same result that produced by NN1. Figure 6.1 and Figure 6.2 shows the results of NN1 (1). Table 6.2 and Table 6.3 describes the model, MSE, initial weights, biased, and the final weights and biased for NN1 (1).

Table 6.2: Scenario 1: description of each model details and MSE results.

Network name	Input features	Number of hidden layers and hidden neurons	MSE training	MSE validation	MSE testing
NN1	Density (ρ)	1	0.0100	0.0174	0.0200
		2	0.0100	0.0174	0.0197
		3	0.0100	0.0174	0.0196
		(3,2)	0.0101	0.0195	0.0215
		(2,2)	0.0100	0.0194	0.0214
	Velocity	1	0.0165	0.0288	0.0411

NN2

Table 6.2 Continued from previous page.

Network name	Input features	Number of hidden layers and hidden neurons	MSE training	MSE validation	MSE testing
		2	0.0165	0.0287	0.0410
		3	0.0165	0.0287	0.0410
		(3,2)	0.0165	0.0288	0.0412
		(2,2)	0.0165	0.0287	0.0411
NN3	Density (ρ) Velocity	1	0.0100	0.0174	0.0200
		2	0.0100	0.0178	0.0206
		3	0.0099	0.0182	0.0215
		(3,2)	0.0100	0.0203	0.0233
		(2,2)	0.0100	0.0202	0.0231
NN4	Velocity Gender Predecessor pedestrian gender	1	0.0165	0.0285	0.0410
		2	0.0165	0.0285	0.0404
		3	0.0165	0.0281	0.0385
		(3,2)	0.0165	0.0286	0.0386
		(2,2)	0.0165	0.0286	0.0406
NN5	Density (ρ) Gender Predecessor pedestrian gender	1	0.0100	0.0172	0.0193
		2	0.0099	0.0170	0.0198
		3	0.0098	0.0170	0.0194
		(3,2)	0.0098	0.0192	0.0221
		(2,2)	0.0099	0.0196	0.0215
NN6	Density (ρ)	1	0.0100	0.0172	0.0192

Table 6.2 Continued from previous page.

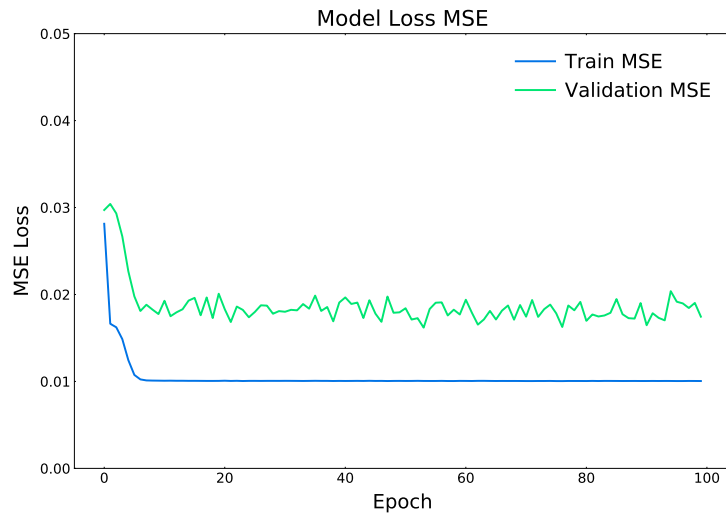| Network name	Input features	Number of hidden layers and hidden neurons	MSE training	MSE validation	MSE testing
	Velocity Gender Predecessor pedestrian gender	2	0.0098	0.0183	0.0202
		3	0.0097	0.0174	0.0204
		(3,2)	0.0097	0.0211	0.0241
		(2,2)	0.0098	0.0210	0.0227

Figure 6.1: The relation between the epochs and the MSE loss at each epoch of model NN1 with one hidden layer and one neuron.

Figure 6.2: The relation between the predicted headway value and the actual value of model NN1 with one hidden layer and one neuron.

Table 6.3: Description of the NN1 (1) weights and bias.

Node	Initial weight	Initial bias	Final weight	Final bias
Hidden layer node	0.62	0	5.33	-1.24
Output layer node	0.59	0	-2.28	0.60

6.4.2 Scenario 2

In Scenario 2, the Palestinian experiments dataset used to predict the velocity and the headway of pedestrians of higher densities. Table 6.4, Figure 6.3, and Figure 6.4 describes the results of Scenario 2.

Table 6.4: Scenario 2: description of each model details and MSE results.

Network name	Input features	Number of hidden layers and hidden neurons	MSE training	MSE validation	MSE testing
NN1	Density (ρ)	1	0.0129	0.0176	0.0302
		2	0.0129	0.0175	0.0301
		3	0.0129	0.0175	0.0301
		(3,2)	0.0129	0.0185	0.0310
		(2,2)	0.0129	0.0184	0.0310
NN5	**Density** (ρ)	1	0.0129	0.0175	0.0300
		2	0.0125	0.0168	0.0284
	Gender	**<u>3</u>**	**<u>0.0117</u>**	**<u>0.0166</u>**	**<u>0.0272</u>**
	Predecessor	**<u>(3,2)</u>**	**<u>0.0118</u>**	**<u>0.0180</u>**	**<u>0.0288</u>**
	pedestrian				
	gender				
		(2,2)	0.0124	0.0177	0.0307

Figure 6.3: The relation between the epochs and the MSE loss at each epoch of model NN5 with one hidden layer and three neurons.
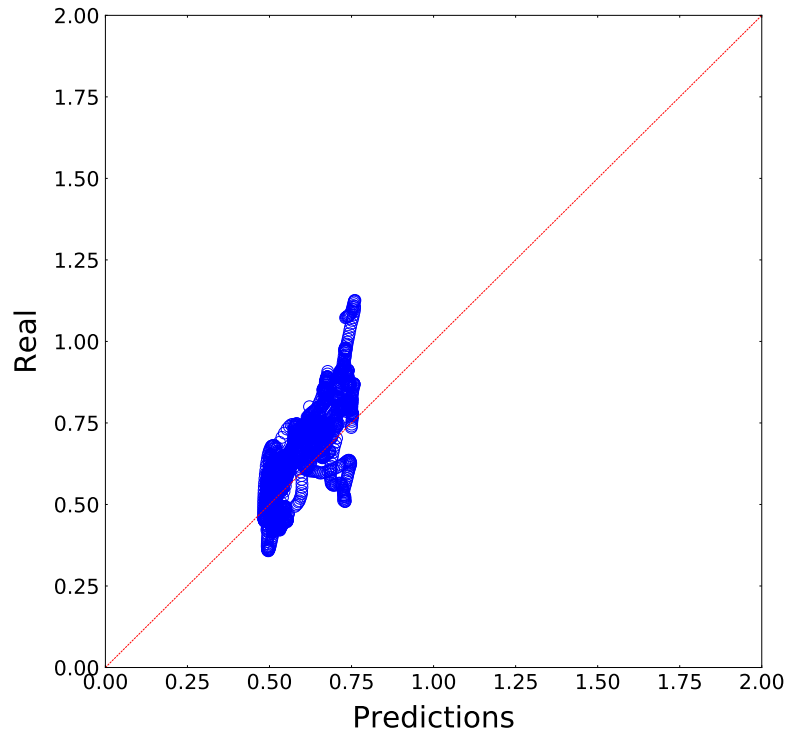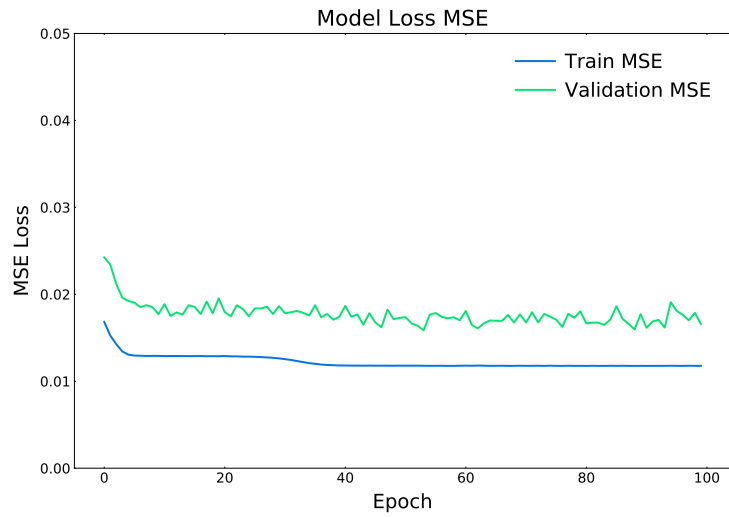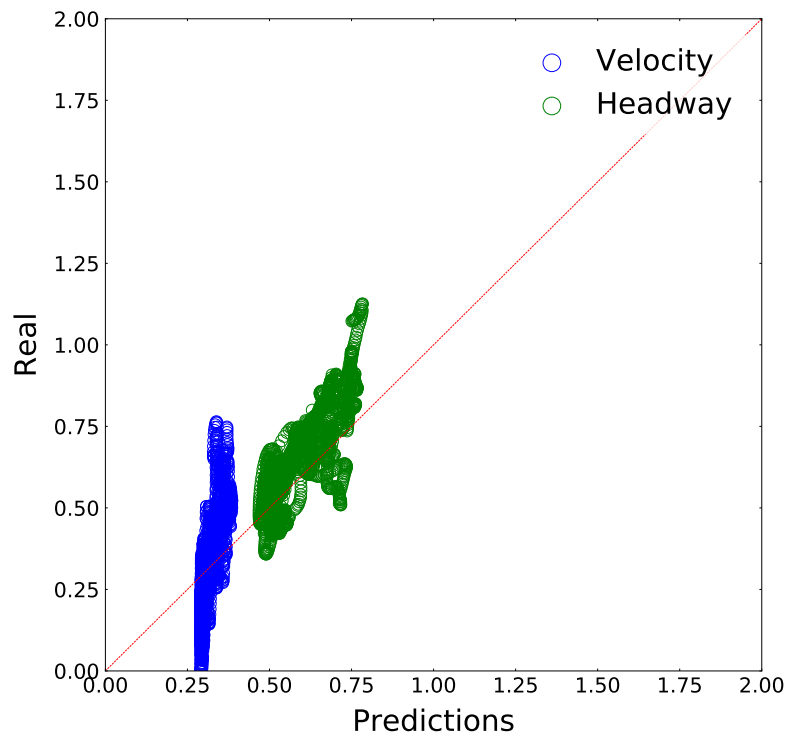

Figure 6.4: The relation between the predicted headway value and the actual value of model NN5 with one hidden layer and three neurons.

6.4.3 Scenario 3.1

In Scenario 3.1, we used the Palestinian experiments dataset as a training and validation datasets to predict the velocity and the headway of Chinese adults on higher densities. Table 6.5, Figure 6.5, and Figure 6.6 describes the results of Scenario 3.1.

Table 6.5: Scenario 3.1: description of each model details and MSE results.

Network name	Input features	Number of hidden layers and hidden neurons	MSE training	MSE validation	MSE testing
NN1	Density (ρ)	1	0.0129	0.0176	0.0241
		2	0.0129	0.0175	0.0245
		3	0.0129	0.0175	0.0245
		(3,2)	0.0129	0.0185	0.0241
		(2,2)	0.0129	0.0184	0.0240
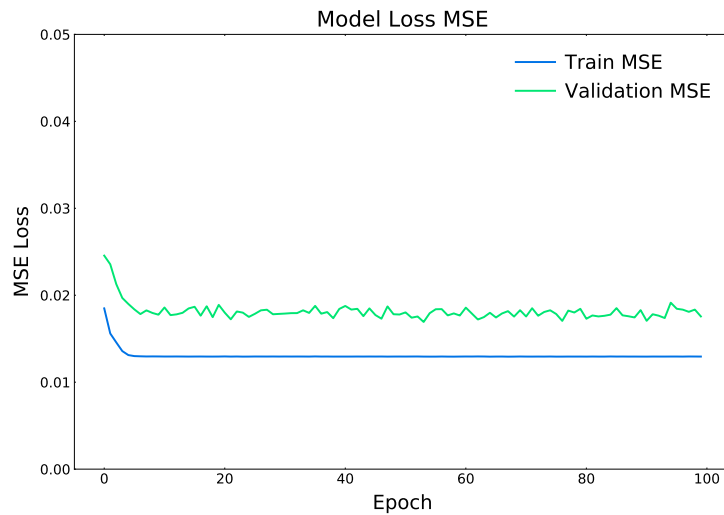
Figure 6.5: The relation between the epochs and the MSE loss at each epoch of model NN1 with one hidden layer and 1 neurons.

Figure 6.6: The relation between the predicted headway value and the actual value of model NN1 with one hidden layer and 1 neuron.

6.4.4   Scenario 3.2

In Scenario 3.2 we used the Palestinian experiments dataset as a training and validation datasets to predict the velocity and the headway of Chinese pedestrians on higher densities. Table 6.6, Figure 6.7, and Figure 6.8 describes the results of Scenario 3.2.

Table 6.6: Scenario 3.2: description of each model details and MSE results.

| Network name	Input features	Number of hidden layers and hidden neurons	MSE training	MSE validation	MSE testing
NN1	Density (ρ)	1	0.0129	0.0176	0.0350
		2	0.0129	0.0175	0.0349
		3	0.0129	0.0175	0.0349
		(3,2)	0.0129	0.0185	0.0357
		(2,2)	0.0129	0.0184	0.0358
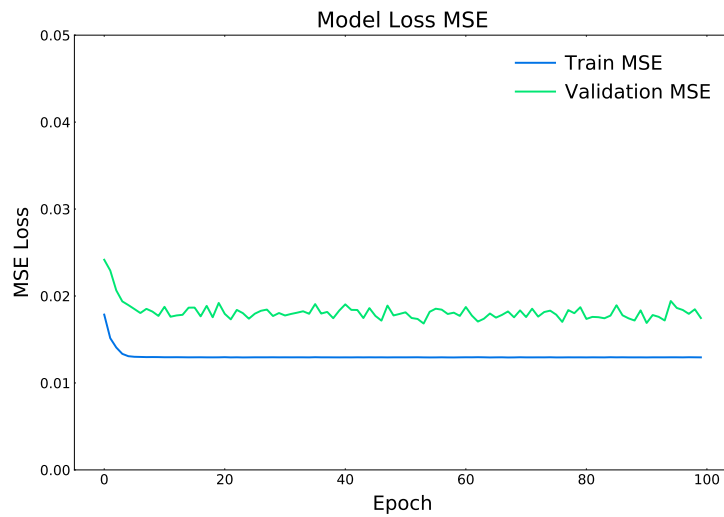
Figure 6.7: The relation between the epochs and the MSE loss at each epoch of model NN1 with one hidden layer and 2 neuron.
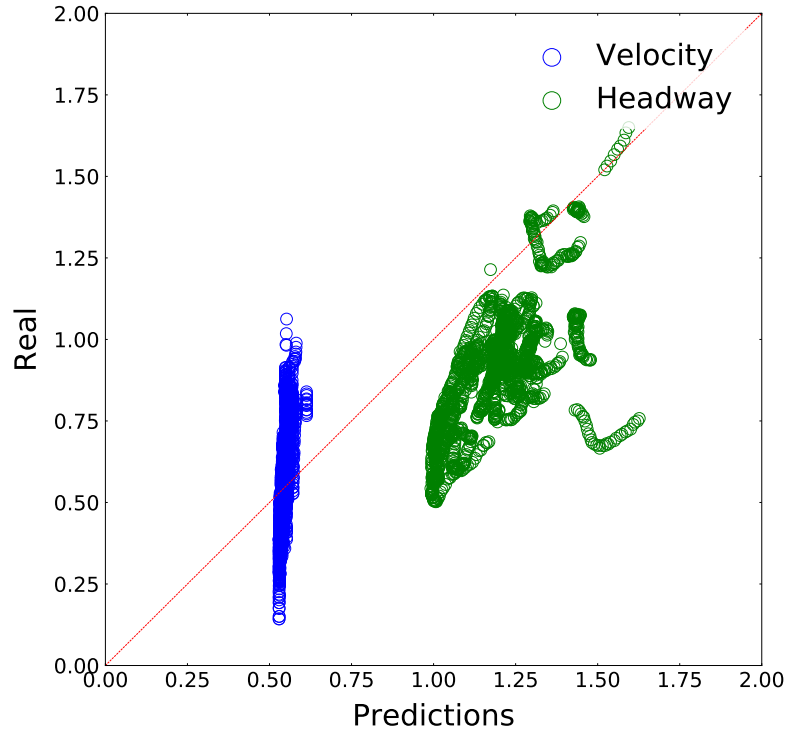
Figure 6.8: The relation between the predicted headway value and the actual value of model NN1 with one hidden layer and 2 neurons.

6.4.5 Scenario 4

In Scenario 4 we used the Palestinian and Chinese (students, adults) experiments dataset as a training and validation dataset to predict the velocity and the headway of Palestinian and Chinese (students, adults) on higher densities. In this scenario, the age fed into the model as input feature with the density. Table 6.7, Figure 6.9, Figure 6.10 describes the results of Scenario 4.

Table 6.7: Scenario 4: description of each model details and MSE results.

| Network name	Input features	Number of hidden layers and hidden neurons	MSE training	MSE validation	MSE testing
	Density (ρ)	1	0.0087	0.0364	0.0583
	Age	2	0.0069	0.0335	0.0435
NN7		**<u>3</u>**	**<u>0.0067</u>**	**<u>0.0325</u>**	**<u>0.0404</u>**
		(3,2)	0.0064	0.0386	0.0459
		(2,2)	0.0065	0.0390	0.0460

Figure 6.9: The relation between the epochs and the MSE loss at each epoch of model NN7 with one hidden layer and 3 neuron.
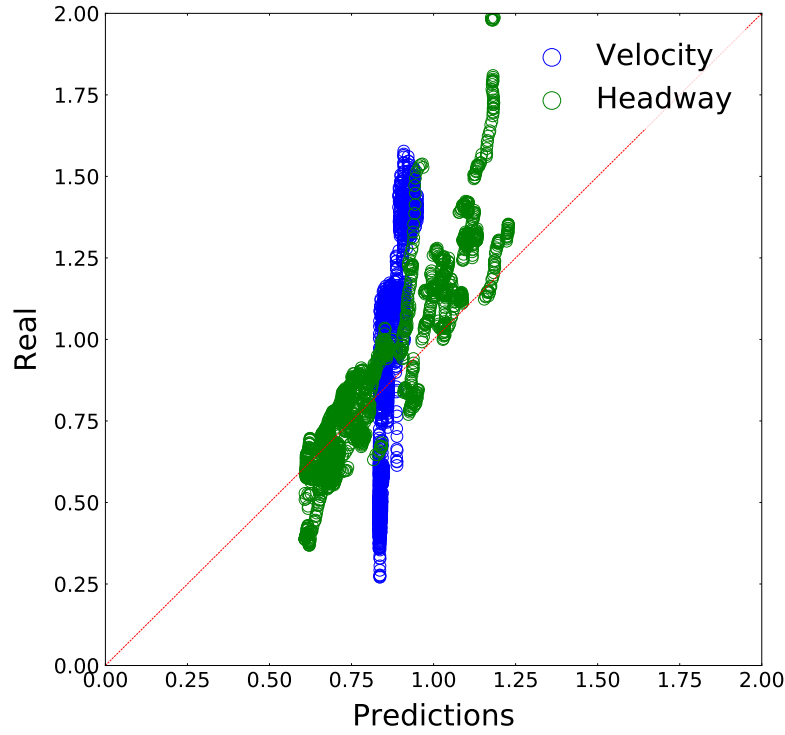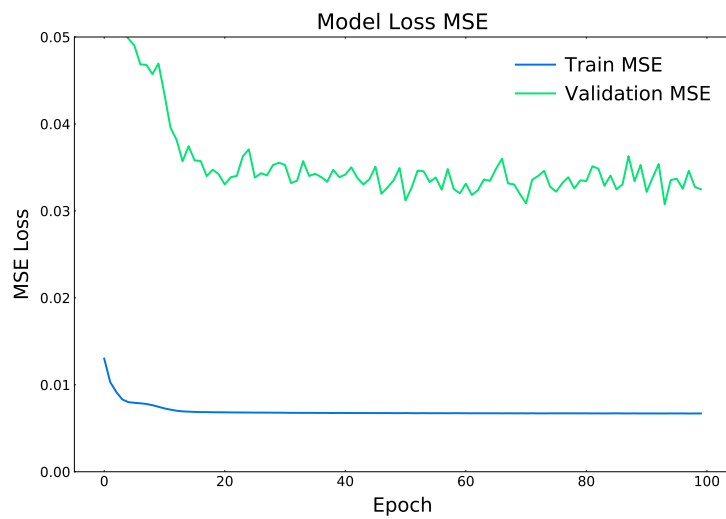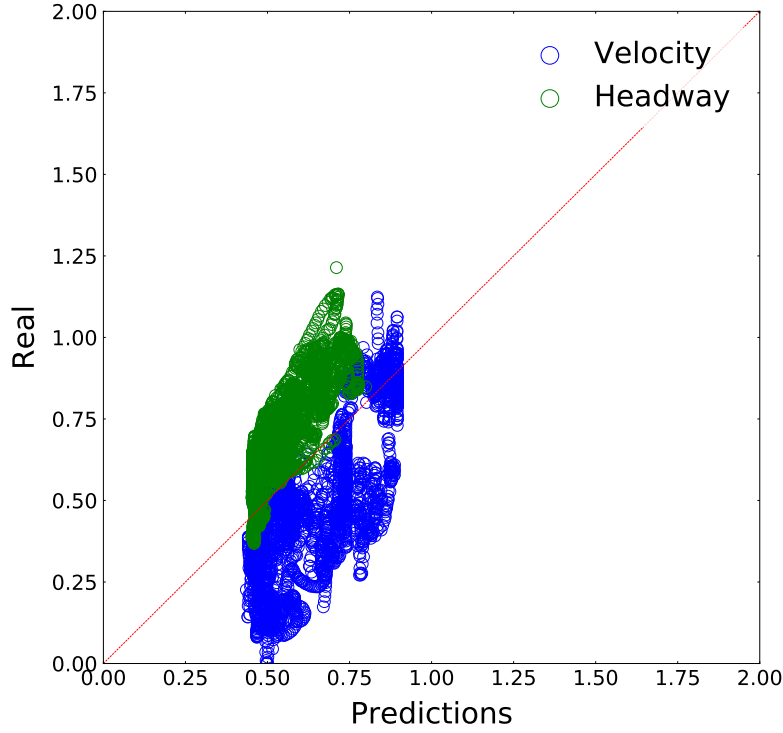
Figure 6.10: The relation between the predicted headway value and the actual value of model NN7 with one hidden layer and 3 neurons.

6.5 Summary

In this chapter, we proposed a prediction model to forecast the velocity and headway of pedestrians specifically of single-file movement set-up. We tried different scenarios by changing the number of hidden layers and the type of input features. The results of Scenario 1 showed that the models with density input features have the best MSE especially in models NN1, NN5, and NN6, and it's enough to use one hidden layer and neuron to predict the headway. For Scenario 2, the results demonstrated that the density with gender information can improve the MSE results specifically when the number of hidden layers is (3,2) and (3). In Scenario 3.1 and 3.2, we predicted the velocity of Chinese students and adults using a model trained using Palestinian data. The results were approximately similar for all cases. Finally, in Scenario 4 the best case to predict the velocity and headway of Chinese and Palestinian using a model trained by their

mixed data was NN7 with (3) hidden layer and neurons.

Chapter 7 — Conclusion, Challenges, and Future Work

In this chapter, we summarize the performed PDs single-file movement experimental results and the proposed pedestrian's movement characteristics prediction model. Also, we discuss the limitations and challenges that we faced while performing the experiments and building our prediction model. In addition, the chapter outlines the future work for the experimental analysis and the proposed prediction model.

In Section 7.1 we present a discussion of the research work contributions and highlight the techniques/ approaches that were utilized in the proposed system. Then, in Section 7.2, we demonstrate the challenges that we faced during our work in the experiments and the proposed prediction model, and we also discuss the future works in the same context.

7.1 Conclusion

In this research work, we presented the results of our single-file movement experiments that have been conducted in Palestine; with an emphasis on various pedestrian compositions. Both male and female students were involved in the experiments. The experiments were filmed and then the trajectory data were extracted from the videos using PeTrack software. Then, we analyzed the main factors that have an impact on PDs characteristics particularly the crowd composition based on gender, social conventions, and age factors by comparing Palestine experimental results with German, India, and China experiments. We have found that with exclusively male and female groups, gender does not affect the pedestrians' movement. For instance, when the number of pedestrians is 20, the velocities for male and female are 0.72 ± 0.10 ms^{-1}and 0.71 ± 0.11 ms^{-1} respectively. Whereas their velocity decreases gradually if they walk in mixed groups with an average velocity of 0.61 ± 0.11 ms^{-1}. Moreover, when the male and female pedestrians walk in a mixed-gender group, they start to reduce their velocities.

According to the social conventions factor, we have found that each culture has it's own mobility properties. For instance, Palestinian pedestrians walk slower than Indian pedestrians and walk besides each other with a smaller comfort zone, and faster than German pedestrians for the same density. Finally, the comparison between Palestine experiments and China experiments confirmed that age has an impact on the dynamics of pedestrians. Elders move slower than the youngest pedestrians for different densities. Surprisingly, it is observed that elder Chinese pedestrians walk faster than the youth pedestrians from Palestine on high densities in mixed experiments. We also proposed a velocity and headway prediction model, exploiting the FFNN approach. Several models presented with a different number of input features, hidden layers, and hidden neurons. The MSE results showed that simple models with a density as input features outperform a more complex model in most cases.

7.2 Challenges and Future Work

Despite the promising results that we have obtained from the experiments and the prediction model, there were still some gaps and challenges that we have faced during our work:

- We performed the single-file movement experiments for males and females in heterogeneous groups with a maximum number of available pedestrians $N = 20$. So, more experimental data are still needed for higher and low densities for both male and female Palestine experiments. This will help in studying the emerging movement behaviors such as the stop and go waves.

- We studied the microscopic and macroscopic movement behavior of pedestrians on single-file movement experiments. But more complex interaction behaviors between Palestinian pedestrians is not investigated yet. So, more types of experiments such as Bottleneck experiments, bi-directional flow corridor experiments, Crossing, 90-degree angle, Crossing, a 120-degree angle, and experiment with obstacles require further exploration. From these experiments, we can study the self-organization phenomena such as Jamming, congestion, lateral swaying (oscillation), and Lane formation ...etc.

- Studying the stepping behavior of pedestrians such as the step length and the step fre-

quency, and compare the results of different gender groups.

- Due to time limitations, we presented a prediction model based on Palestine and Chinese experimental data only to forecast the velocity and headway of the single-file movement set-up. For future work, we plan to build a prediction model to predict more movement quantities using trajectory data and other movement parameters such as the composition of pedestrians and the effect of other neighbors on the pedestrian movement.

References

Alahi, A., Goel, K., Ramanathan, V., Robicquet, A., Fei-Fei, L., & Savarese, S. (2016). Social lstm: Human trajectory prediction in crowded spaces. In *Proceedings of the ieee conference on computer vision and pattern recognition* (pp. 961–971).

Bisagno, N., Garau, N., Montagner, A., & Conci, N. (2019). Virtual crowds: An lstm-based framework for crowd simulation. In *International conference on image analysis and processing* (pp. 117–127).

Boltes, M., & Seyfried, A. (2013). Collecting pedestrian trajectories. *Neurocomputing*, *100*, 127–133.

Boltes, M., Zhang, J., Tordeux, A., Schadschneider, A., & Seyfried, A. (2019). Empirical results of pedestrian and evacuation dynamics. *Complex Dynamics of Traffic Management*, 671–699.

Bürgler, S., & Lindenmann, H. P. (1994). *Ausgeweitete radstreifen bei lichtsignalgesteuerten knoten: Untersuchung des verkehrsablaufes und der verkehrssicherheit* (Tech. Rep.). ETH Zurich.

Cao, S., Zhang, J., Salden, D., Ma, J., Shi, C., & Zhang, R. (2016). Pedestrian dynamics in single-file movement of crowd with different age compositions. *Physical Review E*, *94*(1), 012312.

Cao, S., Zhang, J., Song, W., Shi, C., & Zhang, R. (2018). The stepping behavior analysis of pedestrians from different age groups via a single-file experiment. *Journal of Statistical*

Mechanics: Theory and Experiment, *2018*(3), 033402.

Chattaraj, U., Seyfried, A., & Chakroborty, P. (2009). Comparison of pedestrian fundamental diagram across cultures. *Advances in complex systems*, *12*(03), 393–405.

Das, P., Parida, M., & Katiyar, V. (2015). Analysis of interrelationship between pedestrian flow parameters using artificial neural network. *Journal of Modern Transportation*, *23*(4), 298–309.

Dubroca-Voisin, M., Kabalan, B., & Leurent, F. (2019). On pedestrian traffic management in railway stations: simulation needs and model assessment. *Transportation research procedia*, *37*, 3–10.

Finnis, K. K., & Walton, D. (2008). Field observations to determine the influence of population size, location and individual factors on pedestrian walking speeds. *Ergonomics*, *51*(6), 827–842.

Hasan, I., Setti, F., Tsesmelis, T., Del Bue, A., Galasso, F., & Cristani, M. (2018). Mx-lstm: mixing tracklets and vislets to jointly forecast trajectories and head poses. In *Proceedings of the ieee conference on computer vision and pattern recognition* (pp. 6067–6076).

Heaton, J. (2008). *Introduction to neural networks with java*. Heaton Research, Inc.

Helbing, D., & Molnar, P. (1995). Social force model for pedestrian dynamics. *Physical review E*, *51*(5), 4282.

Jin, C.-J., Jiang, R., Li, R., & Li, D. (2019). Single-file pedestrian flow experiments under high-density conditions. *Physica A: Statistical Mechanics and its Applications*, 121718.

Kuhn, M., & Johnson, K. (2013). *Applied predictive modeling* (Vol. 26). Springer.

Ma, Y., Lee, E. W. M., & Yuen, R. K. K. (2016). An artificial intelligence-based approach for simulating pedestrian movement. *IEEE Transactions on Intelligent Transportation Systems*, *17*(11), 3159–3170.

Morrall, J. F., Ratnayake, L., & Seneviratne, P. (1991). Comparison of central business district pedestrian characteristics in canada and sri lanka. *Transportation Research Record*(1294).

Owaidah, A., Olaru, D., Bennamoun, M., Sohel, F., & Khan, N. (2019). Review of modelling and simulating crowds at mass gathering events: Hajj as a case study. *Journal of Artificial Societies and Social Simulation*, *22*(2), 1–9.

Randhavane, T., Bera, A., Kubin, E., Wang, A., Gray, K., & Manocha, D. (2019). Pedestrian dominance modeling for socially-aware robot navigation. In *2019 international conference on robotics and automation (icra)* (pp. 5621–5628).

Rasouli, A., & Tsotsos, J. K. (2019). Autonomous vehicles that interact with pedestrians: A survey of theory and practice. *IEEE Transactions on Intelligent Transportation Systems*.

Ren, X., Zhang, J., Song, W., & Cao, S. (2019). The fundamental diagrams of elderly pedestrian flow in straight corridors under different densities. *Journal of Statistical Mechanics: Theory and Experiment*, *2019*(2), 023403.

Seyfried, A., Steffen, B., Klingsch, W., & Boltes, M. (2005). The fundamental diagram of pedestrian movement revisited. *Journal of Statistical Mechanics: Theory and Experiment*, *2005*(10), P10002.

Simard, R., & L'Ecuyer, P. (2011). Computing the two-sided kolmogorov-smirnov distribution. *Journal of Statistical Software*, *39*(11), 1–18.

Syed, A., & Morris, B. T. (2019). Sseg-lstm: Semantic scene segmentation for trajectory prediction. In *2019 ieee intelligent vehicles symposium (iv)* (pp. 2504–2509).

Tanaboriboon, Y., & Guyano, J. A. (1991). Analysis of pedestrian movements in bangkok. *Transportation Research Record*, *1294*, 52–56.

Tay, N. C., Connie, T., Ong, T. S., Goh, K. O. M., & Teh, P. S. (2019). A robust abnormal

behavior detection method using convolutional neural network. In *Computational science and technology* (pp. 37–47). Springer.

Tkachuk, K., Song, X., & Maltseva, I. (2018). Application of artificial neural networks for agent-based simulation of emergency evacuation from buildings for various purpose. In *Iop conference series: Materials science and engineering* (Vol. 365, p. 042064).

Tordeux, A., Chraibi, M., Seyfried, A., & Schadschneider, A. (2018). Prediction of pedestrian speed with artificial neural networks. *arXiv preprint arXiv:1801.09782*.

Tordeux, A., Chraibi, M., Seyfried, A., & Schadschneider, A. (2019). Prediction of pedestrian dynamics in complex architectures with artificial neural networks. *Journal of Intelligent Transportation Systems*, 1–13.

Tracker video analysis and modeling tool. (n.d.). `https://physlets.org/tracker/`.

Xiao, Y., Gao, Z., Jiang, R., Li, X., Qu, Y., & Huang, Q. (2019). Investigation of pedestrian dynamics in circle antipode experiments: Analysis and model evaluation with macroscopic indexes. *Transportation Research Part C: Emerging Technologies*, *103*, 174–193.

Xue, H., Huynh, D. Q., & Reynolds, M. (2017). Bi-prediction: pedestrian trajectory prediction based on bidirectional lstm classification. In *2017 international conference on digital image computing: Techniques and applications (dicta)* (pp. 1–8).

Zeng, G., Schadschneider, A., Zhang, J., Wei, S., Song, W., & Ba, R. (2019). Experimental study on the effect of background music on pedestrian movement at high density. *Physics Letters A*, *383*(10), 1011–1018.

Zhang, J. (2012). *Pedestrian fundamental diagrams: Comparative analysis of experiments in different geometries* (Vol. 14). Forschungszentrum Jülich.

Zhang, J., Klingsch, W., Schadschneider, A., & Seyfried, A. (2011). Transitions in pedestrian fundamental diagrams of straight corridors and t-junctions. *Journal of Statistical*

Mechanics: Theory and Experiment, *2011*(06), P06004.

Zhang, J., Mehner, W., Holl, S., Boltes, M., Andresen, E., Schadschneider, A., & Seyfried, A. (2014). Universal flow-density relation of single-file bicycle, pedestrian and car motion. *Physics Letters A*, *378*(44), 3274–3277.

Zhang, P., Ouyang, W., Zhang, P., Xue, J., & Zheng, N. (2019). Sr-lstm: State refinement for lstm towards pedestrian trajectory prediction. In *Proceedings of the ieee conference on computer vision and pattern recognition* (pp. 12085–12094).

الْمُلَخّصْ بِاللّغَةِ العَرَبِية

تَتَأَثَّرْ دِينَامِيكِيّةْ حَرَكَة المُشَاةْ بِالْعَدِيد مِنَ الْعَوَامِلْ التِي تُشَكّلْ خَصَائِصَهَا الْمُخْتَلِفَة مِثْل التَّدَفُقْ، السُّرْعَة، والْكَثَافَة فِي مَجمُوعَاتْ المُشَاةْ الْمُخْتَلِفَة. بَعْض هَذِه الْعَوَامِلْ لَهُ عَلَاقَة بِتَرْكِيبَةْ حُشُودْ المُشَاة. لِذَلِكَ تُعْتَبَر التَّجَارُبْ اَلتِي تُرَكّز عَلَى دِرَاسَةْ حَرَكَة المُشَاة فِي الْمَمَرَّاتِ الَّضِّيقَة فِي ظُرُوفٍ مَخْبَرِيّة مُخْتَلِفَة مِنْ أَهَمْ تَجَارُبْ دِينَامِيكِيّةْ حَرَكَةِ المُشَاةْ. تَتَمَثَّلْ الْفَائِدَة مِنْ هَذَاَ الْنَوْعْ مِنَ الْتَجَارُبْ الْمُبَسَّطَة بِسُهُولَةِ الْتَحَكُمْ فِي كَثَافَةْ وَعَدَدْ الْأَشْخَاصْ فِيهَا، والَّذِي يَسْمَحْ بِدِرَاسَةْ النَّمُوذَجْ أَلْأَسَاسِي (العَلاَقَة مَا بَيْن الكَثَافَة والسُّرْعَة) بِطَرِيقَة مَضْبُوطَة وَمُنَّسِقَة. الْهَدَفْ مِنْ هَذَا الْبَحْثْ هُوَ اسْتَكْشَافْ وَدِرَاسَةْ خَصَائِصْ حَرَكَةِ المُشَاةْ بِنَاءً عَلَى تَجَارُبْ "حَرَكَة المُشَاةْ الْفَرْدِيَّة" تَمَ تَنْفِيذَهَا فِي فَلَسْطِينْ بِالْتَرْكِيزْ عَلَى جِنْسْ المُشَاةْ (ذُكُورْ، إنَاثْ) مِنْ خِلَالْ دِرَاسَةْ الْعَلَاقَة مَا بَيْنْ الْكَثَافَة والسُّرْعَة، مَسَافَة الْتَقَدُّمْ والسُّرْعَة، وَكَثَافَةِ المُشَاةْ والسُّرْعَة. وَمِنْ ثُمَ مُقَارَنَةْ نَتَائِجْ هَذِه الْتَجَارُبْ الِّتِي تَمَ الْتَوَصُّلْ إلَيْهَا مَعَ تَجَارُبْ الْحَرَكَة الْفَرْدِيَّة فِي الْبُلْدَانْ الْأُخْرَى مِثْلْ أَلْمَانْيَا والهِنْدْ. أَيْضاً قُمْنَا بِإِجْرَاءَ مُقَارَنَة تَحْلِيلِيّة تُرَكِّزْ عَلَى عَامِلْ الْعُمْرْ وَكَيْفِيَةْ تَأْثِيرِه عَلَى خَصَائِصْ حَرَكَةِ المُشَاةْ الْمُخْتَلِفَة، وَذَلِكَ مِنْ خِلَالْ دِرَاسَةْ الْفِئَاتْ الْعُمْرِيّة الْتَالِيَة: الْشَبَابْ بِعُمْرْ الْـ 19 عَاماً (تَجْرِبَة فِلَسْطِينْ)، الْشَبَابْ بِعُمْرْ الْـ 17 عَاماً (تَجْرُبَةْ الْصِّينْ)، والْكُهُولْ بِعُمْرْ الْـ 52 عَاماً (تَجْرُبَةْ الْصِّينْ). بَعْدَ تَحْدِيدِ الْعَوَامِلْ الْمُؤَثِّرَة عَلَى دِينَامِيكِيّة حَرَكَةِ المُشَاةْ، قُمْنَا بِاسْتِخْدَامِهَا فِي دِرَاسَةِ تَأْثِيرِهَا فِي الْعَوَامِلْ الْأُخْرَى الْمَسْؤُولَة عَنْ اتِّخَاذْ الْقَرَارْ فِي الْحَرَكَة الْمُسْتَقْبَلِيّة، وَتَوَقُّعْ الْخَصَائِصْ الْمُسْتَقْبَلِيّة لِلمُشَاة بِاسْتِخْدَامْ الذَّكَاءْ الْإصْطِنَاعِي (الْشَبَكَاتْ الْعَصَبِيّة الْصِنَاعِيَّة).